

Role of Charge–carrier Trapping in Organic Optoelectronic Devices[†]

IRENEUSZ GLOWACKI*, JAROSLAW JUNG, GABRIELA WIOSNA–SALYGA,
MARIAN CHAPRAN, ADAM LUCZAK, BERTRAND G. R. DUPONT,
BEATA LUSZCZYNSKA AND JACEK ULANSKI

*Department of Molecular Physics, Lodz University of Technology,
Zeromskiego 116, 90–924 Lodz, Poland*

Received: October 26, 2016. Accepted: January 25, 2017.

This review aims to analyse the impact of charge carrier trapping processes on the performance of organic optoelectronic devices, particularly organic light emitting diodes. The importance of this subject stems from the fact that the trapping processes are unavoidable in organic semiconductors. The photogeneration, transport and recombination of charge carriers are affected by the presence of traps. In the introduction, after a brief presentation of the basic equations describing the kinetic of charge carrier trapping in semiconductors, the working principles of the organic light emitting diodes, organic photovoltaics and organic thin film transistors will be described in elementary terms. Specifically, the reason for the trapping processes and how they manifest themselves in such devices will be investigated. In the second part of the paper, the most important experimental techniques used for the detection and the characterization of the charge carrier traps in organic semiconductors will be described. Finally, in the last part of the review, the state-of-the-art research on the origin, the mechanisms and the role of the trapping phenomena observed experimentally in working organic optoelectronic devices, will be presented.

Keywords: charge carrier trapping, organic light emitting diode, organic photovoltaic device, organic field effect transistor

*Corresponding author: ireneusz.glowacki@p.lodz.pl

[†]The research leading to these results received funding from the H2020-MSCA-ITN-2015/674990 project “EXCILIGHT”.

1. INTRODUCTION

Charge trapping phenomena in:

1.1. Organic semiconductors (general consideration)

Charge carrier trapping processes are unavoidable in organic semiconductors, with the exception of extremely pure and defect-free single crystals. Trapping sites in organic semiconductors may have various origins; they can be formed by structural defects (resulting in local positional or energetical disorder), dipoles, excimers, or guest molecules (impurities or dopants). Charge carrier trapping usually limits the charge carrier transport properties of materials, however trapping may also affect, directly or indirectly, the processes of photogeneration and recombination of charge carriers. For these reasons, charge carrier trapping effects should always be taken into account in the analysis of the performance of electronic devices, such as organic light emitting diodes (OLEDs), organic photovoltaic devices (OPVs) or organic field effect transistors (OFETs) [1].

The kinetics of the trapping is given by the following equation [2]:

$$\frac{dn_t}{dt} = k_1 n (N_t - n_t) \quad (1)$$

where: n_t is the filled trap concentration, k_1 is the rate constant of trapping, n is the concentration of free charge carriers, and N_t is the trap concentration. For a low concentration of filled traps ($n_t \ll N_t$), the trapping rate is given by:

$$\frac{dn_t}{dt} = \frac{n}{\tau} \quad (2)$$

where: τ is the mean lifetime of the free charge carriers expressed as:

$$\tau = \frac{1}{N_t \Lambda v} \quad (3)$$

where: Λ is the trapping cross-section and v is the mean velocity of the free charge carriers.

The detrapping rate is then given by:

$$\frac{dn_t}{dt} = k_2 n_t (N_c - n) \quad (4)$$

where: N_c is the concentration of transporting sites, and the constant rate of detrapping k_2 for equilibrium conditions is determined by the Fermi statistics:

$$k_2 = k_1 \exp\left(\frac{E_t}{k_B T}\right) \quad (5)$$

where: E_t is the trap depth, k_B is the Boltzmann constant and T is the temperature.

Hoesterey and Letson [3] elaborated a model describing how the carrier mobility in anthracene crystals decreases with the increase of the energetical traps depth E_t , and the trap concentration c :

$$\mu = \frac{\mu_0}{1 + c \exp\left(\frac{E_t}{k_B T}\right)} \quad (6)$$

where: μ_0 is the mobility of the charge carriers in the crystal without traps.

Using as an example anthracene, a single crystal containing well-defined additives such as: anthraquinone, anthrone or naphthacene, they presented the trapping operations in this model.

Such a classical approach to the trapping and detrapping processes usually does not reflect properly the much more complex phenomena which occur in a disordered organic semiconductor, in particular when working with organic electronic devices, where the active layers may have a very different morphology (amorphous or polycrystalline, isotropic or oriented, in the form of ultra-thin layers, multi-layered laminates or multicomponent composites, etc.), and where the current density is usually relatively high.

It should be underlined that in the vast majority of organic materials the transport of charge carriers is dominated by the transport of holes (the electron mobility is much lower than the hole mobility). As pointed out by Köhler and Bässler [1], a low electron mobility in the molecular materials can be explained by the presence of oxygen or the oxidation products with a lowest unoccupied molecular orbital (LUMO) lower than that of the one of the host. A universal character of the electron trapping sites bearing a LUMO at ca -3.6 eV relative to the vacuum level in conjugated polymers was assigned to the common presence of hydrated oxygen complexes [4]. The depth of the traps created by the dopants depends on the difference between the highest occupied molecular orbital (HOMO) levels (for holes) and the LUMO levels (for electrons) of the matrix and of the dopant molecules.

A high concentration of trapped charge carriers would lead to the modification of the internal electric field in the active layers of devices. At a high current density the tail states of the DOS (density of states) are partially occupied, shifting up the quasi-Fermi level, and hence the charge carriers would reach the level of transport energy more efficiently and their mobility would increase [1]. It explains, why the charge carrier mobility determined from the characteristics of OFETs can be much higher than the mobility measured by

time-of-flight methods [1]. We are referring the reader to an excellent discussion of these problems in the book by Köhler and Bässler [1].

Moreover, in the case of polymer materials, one must take into account the molecular relaxations of the polymer chain segments. It was found, that the detrapping of charge carriers may be induced by the molecular relaxations which also occur in glassy (so nominally solid) state. Such an effect (called ‘wet dog’ effect) was explained by the assumption that the thermally activated molecular relaxations may facilitate the inter-site hopping of charge carriers by lowering the potential barriers of the trapping sites or by decreasing the distance between the neighbouring localized sites [5].

1.2. Organic Light Emitting Diodes (OLEDs)

The working principle of light emitting diodes is based on the generation of excitons (Fig. 1). When an electric field is applied between electrodes, electrons and holes are injected into the organic semiconductor, which serves as an active layer for the LED. Charges are transported, trapped and when electron and hole meet each other, an exciton is created. When the opposite charges recombine radiatively, a light of a certain colour is emitted (see Fig. 1(b)).

The colour of the emitted light depends on (but is not directly equal to) the energy difference between HOMO and LUMO levels of the electroluminescent molecule. It is important to know that the light colour is substantially related to the energy of the emissive state (singlet or triplet). The energy states refer to the total energy and overall electron configuration of the whole molecule, whereas orbitals describe the location and energy of electrons in a specific orbital.

As a result of the electron-hole interaction singlet or triplet excitons can be generated however according to the spin statistic the population of triplets is three times higher than the singlets’ one. Consequently, in the case of the fluorescent organic emitters only up to 25% of the total number of excitons

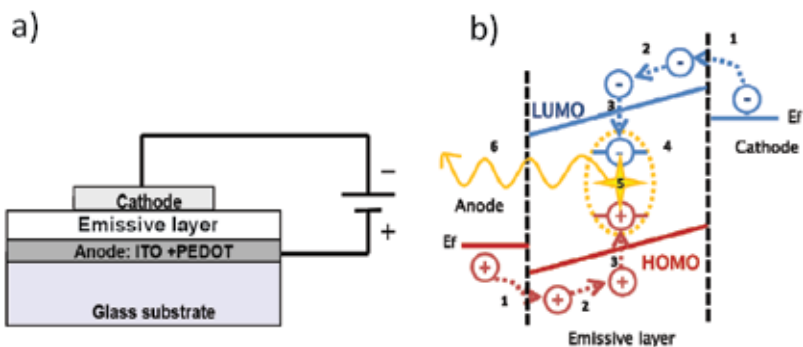


FIGURE 1

a) Simplest sandwich structure of an OLED, b) Energy level diagram and scheme of occurring processes in a forward bias OLED: 1. Charge carrier injection, 2. Charge carrier transport, 3. Charge carrier trapping, 4. Exciton creation, 5. Radiative exciton recombination.

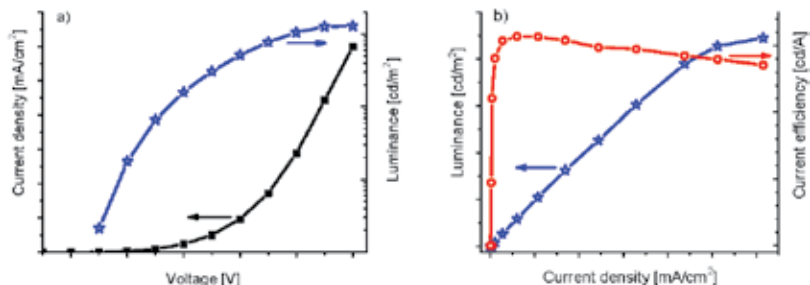


FIGURE 2
a) Typical I - V - L characteristics of OLEDs and b) luminance and current efficiency versus current density.

can be exploited in OLEDs. To avoid this limitation phosphorescent, or exciplex emitters are applied in OLEDs since theoretically, this should allow gaining in emission from all created excitons.

Several parameters are used to characterize the efficiency of OLEDs. These are current (luminous) efficiency, power efficiency and quantum efficiency. In the evaluation of OLEDs, the current efficiency (η_A) is very important. It represents the ratio of the luminance (L) to the current density (j) flowing through the diode and is expressed in cd/A. The typical current-voltage-luminance (I - V - L) characteristics and the luminance-current density-current efficiency dependencies of OLEDs are shown in Fig. 2. The increase in the current density causes the initial rapid increase in the current efficiency however after reaching a maximum value it begins to decrease with increasing values of the current flowing through the diode (see Fig. 2(b)) [6, 7]. The operating parameters of OLEDs are affected by many factors, and one of them is the presence of traps in the emission layer.

In real OLEDs, as well as in other organic devices, the transport process will depend not only on the electronic properties of the semiconductor molecules, but also on the supramolecular structure (morphology) of the active layers. The morphology of the active layer strongly depends on the preparation method. The formation of different crystalline structures and of amorphous phases will affect the density of transport states and traps.

The presence of traps hinders the charge carrier transport in the OLEDs and higher operation voltages have to be applied. The injected carriers will gradually fill the traps. One can therefore observe a higher threshold voltage and a steeper increase in the current density and the intensity of the emitted light [6, 7].

The trapping states have various origins and characters. The traps can be formed by the matrix materials but also by the introduced emitter molecules that may create new traps. The position of the HOMO and the LUMO energy levels of the dopants, relating to the energy levels of the matrix, will determine the type as well as the depth of the formed traps (Fig. 3) [8].

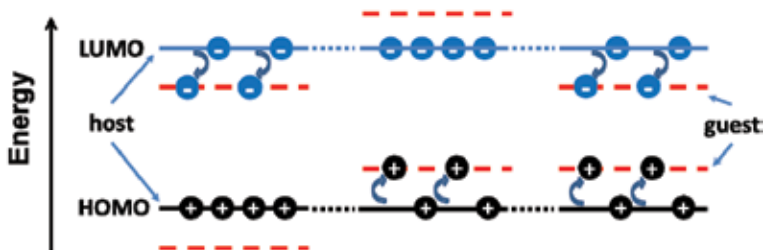


FIGURE 3

Three types of carrier trapping in the host–guest systems. From left to right: (a) electron trapping, (b) hole trapping, and (c) both electron and hole trapping.

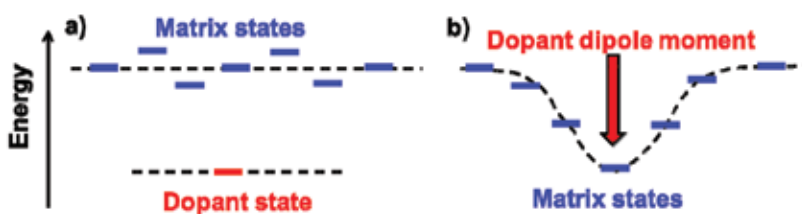


FIGURE 4

Energy levels in the host–guest system when the guest molecule creates a deep charge trap (a); and situation when a strong dipole moment of a guest molecule causes the lowering of the energy of the host sites (b).

Moreover, a dopant molecule with a high dipole moment could reshape the surrounding electrostatic landscape due to the charge–dipole interactions. Hence, the energy of some sites of the matrix localised in the neighbourhood of the guest could be lowered and these sites might work as deeper traps when compared to those in the neat matrix (Fig. 4).

The effects of the polar additives on the transport process in the disordered molecular solids were analysed by many research groups [9–12].

Such introduced dopant molecules may also compete with the one existing in the matrix (traps or recombination centres) and may affect the performance and the spectrum of the electroluminescence. The trapped carriers can quench the excited states and reduce the efficiency of the electroluminescence. On the other hand, they may also contribute to the generation of new excitons resulting in an increase of the emission in the OLEDs. That is why the process of charge carriers trapping in the emissive layers is one of the important factor affecting the generation of light quanta in the OLEDs [13].

1.3. Organic Photovoltaic Devices (OPVs)

The exciton diffusion range is in most organic semiconductors very short, usually below 10 nm. In order to create a photovoltaic effect the excitons should reach the donor–acceptor interface to facilitate the dissociation of

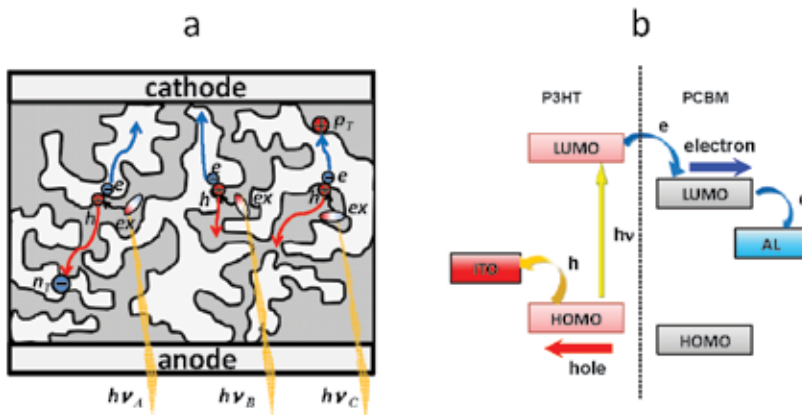


FIGURE 5

a) Schematic structure of a bulk heterojunction made of interpenetrating networks of donor-type (grey), and acceptor-type (white) phases. The symbol *ex* designates the excitons, *hν* – the light quantum, *e* – the electrons, *h* – the holes, and *n_T* and *p_T* the concentrations of charged traps for electrons and holes, respectively. b) Schematic diagram of the photogeneration of holes and electrons in a P3HT/PCBM BHJ system [15].

bounded electrons and holes and then the transfer of the free electrons to the acceptor material and of the holes to the donor material. Usually, the thickness of the semiconductor layer has to be much larger (more than 100 nm) to assure an effective sun light absorption. To overcome these contradictory requirements, a nanoscale interpenetrating and bi-continuous networks of donor and acceptor has to be formed: the so-called bulk heterojunction (BHJ) [14]. A schematic cross-section of an organic photovoltaic device (OPV) with BHJ is shown in Fig. 5.

In the BHJ system, the interpenetrating phases of semiconductors with a *p*-type conductivity (e.g. P3HT) and an *n*-type conductivity (e.g. PCBM) are forming a *p-n* junction with a large interface surface. Due to such a morphology, the thickness of the BHJ layer can even be over 100 nm thick, but the excitons have to diffuse through a much shorter distance to reach the *p-n* interface where they can dissociate into free holes and electrons, as shown schematically in Fig. 5(a). Then the holes are transported to the anode *via* a *p*-type phase and the electrons to the cathode *via* an *n*-type phase.

In order to reduce the formation of barriers at the interface between the electrodes and BHJ layer, the anode should be made of a conductor with a work function adjusted to the HOMO level donor-type semiconductor, and the cathode material should have a work function adjusted to the LUMO level of the acceptor-type semiconductor (Fig. 5(b)).

Under illumination, if the electrodes of the OPV device are not short-circuited, an open-circuit voltage, *V_{oc}*, will be created between the anode and cathode. When the electrodes are short-circuited, a short-circuit current, *I_{sc}*,

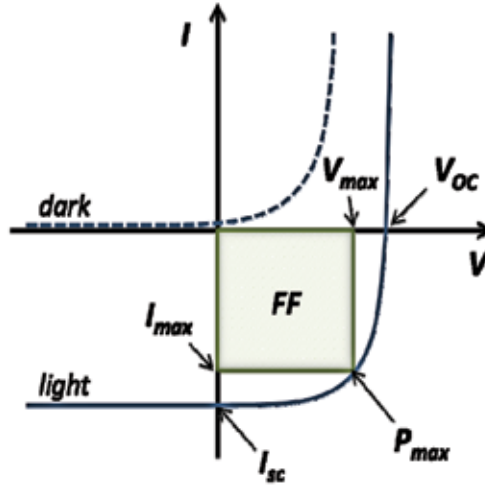


FIGURE 6

Typical current–voltage characteristics of an OPV in the dark and under illumination and basic parameters of the OPVs: maximum power (P_{\max}), fill factor (FF).

will flow in the external circuit. Fig. 6 illustrates the model current–voltage characteristics of an OPV in the dark and under illumination as well as the basic parameters of OPV. Following are their respective equations:

$$P_{\max} = I_{\max} V_{\max} \quad (7)$$

$$FF = \frac{P_{\max}}{I_{sc} V_{oc}} \quad (8)$$

$$PCE = \frac{P_{\max}}{P_{ph}} \quad (9)$$

where: P_{ph} designates incident radiant energy.

The most important phenomenon influencing the performance of the OPV are the photogeneration, recombination and transport of the charge carriers. These can be strongly affected by the trapping states existing between the HOMO and the LUMO levels. Especially in the heterogeneous BHJ composites, the created positional and energetic disorder promotes the formation of new trapping sites. The trapped charge carriers may hinder the diffusion of the excitons and cause their quenching [16]. The space charge formed by the

charged traps would significantly reduce the build-in an electric field [17], leading to a reduced drift velocity of the charge carriers and the increased probability of bimolecular recombination [18]. Each of these phenomena results in the reduction of the basic parameters of the OPVs (P_{\max} , FF , V_{oc} , I_{sc}) which determine the efficiency of the energy conversion of light into electricity.

1.4. Organic thin-film field effect transistors (OTFT)

While the role of light-emitting diodes and photovoltaic cells is to efficiently exchange the energy between the electricity and the light, transistors are used to control the flow of charge carriers. The organic thin-film field effect transistors (OTFT), schematically presented in Fig. 7, comprise an organic semiconductor layer in which the current flow between the source and the drain electrodes and is controlled by a potential applied to the isolated electrode, the gate. The drain current intensity depends on several conditions such as: the voltage applied to the electrodes, the materials used in the devices, the methods used for the preparation of OTFT and the architecture of the OTFT.

The field-effect-transistors principle consist in controlling the drain current I_{DS} by modulating the gate-source applied voltage V_{GS} . The voltage applied to the gate creates an electric field in the dielectric which attracts the charge carriers present in the semiconductor to the semiconductor/dielectric interface. In effect, in the very thin layer of the semiconductor, next to the dielectric, a conducting channel is created. When a potential difference, V_{DS} , is applied to the drain and source electrodes, a drain current, I_{DS} , is flowing, and since the density of charge carriers in the conducting channel depends on the applied voltage V_{DS} , the drain current intensity also depends on V_{GS} .

Figure 8 shows the so-called output $I_{DS}(V_{DS})$ and transient $I_{DS}(V_{GS})$ current-voltage characteristics for a hypothetical field-effect-transistor with an

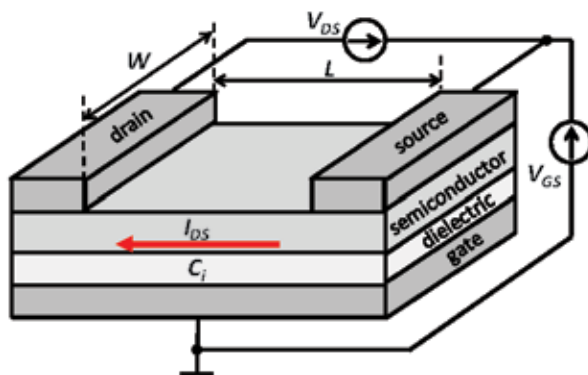


FIGURE 7

Scheme of an OTFT with a bottom gate and a top contacts (BGTC) configuration; W – width of the channel; L – length of the channel; C_i – capacitance of the gate dielectric; I_{DS} – drain current, V_{GS} – gate-source applied voltage; V_{DS} – drain-source applied voltage.

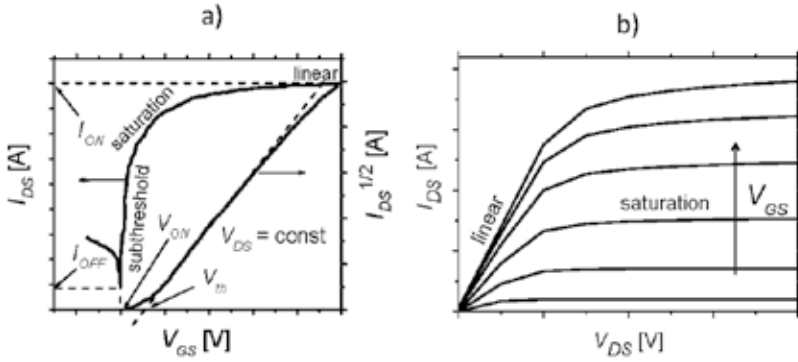


FIGURE 8

Current–voltage transient a) and output b) characteristics for field–effect transistor with an n -type channel with the determination methods of basic parameters such as: V_{th} , V_{ON} , I_{ON} and I_{OFF} .

n -type channel and with indicated ranges: subthreshold, linear and saturation. Such representations of the current–voltage characteristics allow the determination of the basic parameters of the transistor needed to design functional electronic circuits: charge carrier mobility μ_{FET} , threshold voltage V_{th} , switch on voltage V_{ON} , ON/OFF ratio and subthreshold swing SS .

The parameters of an OTFT such as: μ_{FET} , ON/OFF and SS are calculated according to the following formulas:

$$\mu_{FET} = \frac{2L}{WC_i} \left(\frac{\partial \sqrt{I_{DS}}}{\partial V_{GS}} \right)^2 \quad \text{for } V_{GS} > V_{th} \quad (10)$$

$$ON/OFF = \frac{I_{ON}}{I_{OFF}} \quad (11)$$

$$SS = \frac{dV_{GS}}{d(\log(I_{DS}))} \quad \text{for } V_{GS} < V_{th} \quad (12)$$

From an application point of view, it is indispensable to have transistors with μ_{FET} , ON/OFF and SS values as high as possible, while the V_{th} and V_{ON} values should be very low. Furthermore, the long term stability of these parameters is important factors impacting the quality of the devices.

Since the operation of OFETs depends on the current flow, the charge carrier trapping influences directly its performance. In organic semiconductor layers, there are many potential sources for trapping sites such as: morphological inhomogeneities, defects, impurities and interfaces. Low molecular weight organic

semiconductors usually form polycrystalline, granular structures, and charge carriers can be trapped at the inter-grain boundaries, as well as at dislocations and at impurities inside the grains. Layers made of semiconducting polymers are even more disordered, comprising both a crystalline and an amorphous phase, with a broad distribution of molecular weight and conjugation length. Charge carriers are also often trapped at the semiconductor/dielectric interface, due to different impurities adsorbed at the interface (like hydrated oxygen complexes) or are pinned by dipoles in the dielectric [16, 17].

2. EXPERIMENTAL TECHNIQUES FOR THE CHARACTERISATION OF THE TRAPPING PHENOMENON

The charge carrier trapping phenomenon may have an impact on all electronic processes observed in semiconductors, therefore the trapping manifests itself in the measurements of different electronic or opto-electronic properties of organic semiconductors. Many charge carrier traps investigation techniques have been developed over the years such as, deep-level transient spectroscopy (DLTS), impedance spectroscopy [18], thermally stimulated capacitance, or the admittance spectroscopy technique [19]. Among them, the DLTS is regarded as particularly useful, because it is a sensitive, rapid, and easy analysis method. The DLTS technique is a high-frequency capacitance transient thermal scanning technique, able to distinguish between the majority and the minority carrier traps and can provide information about the concentration, energy levels, and electron and hole capture cross sections of traps [20].

Other spectroscopic methods for the determination of the traps depth, further mentioned in section 2.2 and also used for semiconducting polymers, are the photothermal deflection spectroscopy and the internal photo-emission spectroscopy [21].

One should however note that none of these techniques have so far found wider applications for the investigation of organic semiconductors. In most cases, authors only mention evidence of the presence of charge trapping, but these do not allow the determination of the parameters of the traps. There are only a few techniques which give more detailed information on the trapping processes [22]. The most important of these will be described thereafter.

2.1. Thermally Stimulated Currents and Thermoluminescence Techniques

The most direct methods for the characterisation of charge carrier traps in semiconductors and dielectrics consist in the observation of the effects of the thermal activation of the detrapping. These either consist of an increase of the flowing current in the thermally stimulated currents (TSC), or of a radiative recombination in the thermoluminescence (TL) [23–27]. Diagrams illustrating the TSC and TL procedures are shown in Fig. 9.

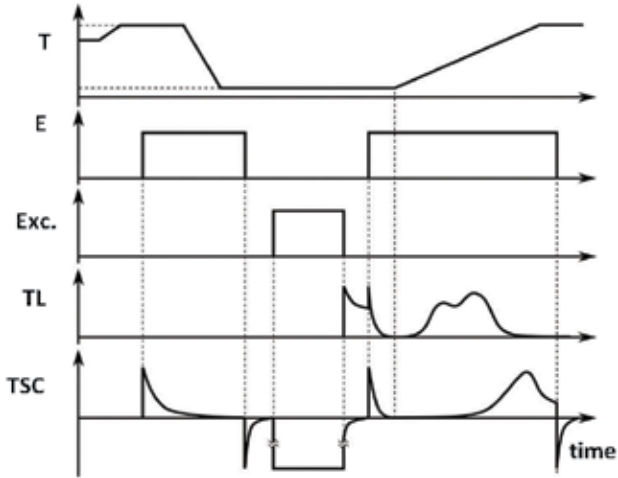


FIGURE 9

Diagram illustrating the simultaneous measurements of TSC and TL; T – temperature; E – electric field; Exc. – photoexcitation; TL – thermoluminescence signal; TSC – thermally stimulated current.

In the first step of the procedure, the sample is cooled down to a low temperature. Then the traps have to be filled by the charge carriers which can be photogenerated or injected from the electrodes. The sample is further heated up, usually at a constant rate, in order to release the trapped charge carriers. In the TSC experiment, this phenomenon is translated as an increase of the measured current flowing under an applied constant and a low extracting electric field. In the TL experiment, one can detect an increase in the intensity of the emitted light resulting from the geminate recombination of the photo-generated electron–hole pairs. With the increasing of the temperature the concentration of the liberated charge carriers initially increases, but then at a certain temperature, due to a decreased concentration of trapped charge carriers, the liberated charge carriers start to decrease in concentration. This leads to a maximum visualised in the TSC or in the TL spectra. Generally, the T_{max} temperature, at which the TSC or TL maximum is observed, is influenced by the depth of the traps. As a first approach this depth (E_t) was determined from the following simple relation [28]:

$$E_t = \frac{T_{max}}{400} \quad (13)$$

However, such an approximation can only be used for materials in which the traps are neutral, with a narrow distribution of the energetic depth, where the charge carriers show a high mobility and retrapping is negligible. In most organic semiconductors, such conditions are not fulfilled.

In materials with low charge carrier mobility, the position of the TSC maximum is not only dependent on the depth of the traps, but also on the transit time required for the transport of the detrapped charge carriers travelling towards the electrode. The position of the maximum will therefore shift towards lower temperatures with increasing extracting electric field applied during the experiment [29]. In some cases, one could treat the TSC maxima as the thermally activated Time-of-Flight signals [30] in which are sometime called in the literature: “the TSC transport maxima” [31].

In the TL experiment, the external electric field does not affect the position of the TL maximum (under the neutral traps assumption), because the geminate recombination appears immediately after the liberation of the charge carriers from the traps. However, an increased electric field will involve the highest probability that the liberated charge carrier would avoid geminated recombination. And indeed, in a series of simultaneous TSC and TL experiments performed on several poly(N-vinylcarbazole)/polycarbonate blends, it was found that the position of the TL maximum remained unchanged with an increased electric field while its intensity decreased at the same time. Meanwhile, the TSC maxima was also shown to grow and move to lower temperatures [29].

The situation is however more complex for the charged-when-empty traps. This is because the external electric field leads to the lowering of the Coulomb potential barrier which means an apparent decrease of the trap depth: the so-called Poole-Frenkel effect [32]. Hence, with an increased electric field both the TSC and the TL maxima will shift towards lower temperatures. Because the Poole-Frenkel approach is a simplified quasi 1-dimensional model, the effect for a realistic 3-dimensional disordered material has to be analysed using the Onsager model of geminate recombination. This involves a rather difficult analysis of the TSC and TL spectra [33].

Fortunately, the TL experiments do not require the use of an electric field, and are usually performed on samples without any electrodes. The drawback of the TL technique is that it is limited to materials showing a radiative charge carrier recombination. It is however suitable for the emitting layers used in OLEDs.

Due to the broad distribution of the trap states energy in disordered materials, the TL and TSC spectra display broad and unstructured maxima. Such overlapped maxima can be resolved using the so-called ‘partial heating’ technique [27, 29]. In this technique, the sample is heated to a T_1 temperature well below the maximum temperature T_{\max} ($T_1 \ll T_{\max}$), and the emitted light intensity (in TL) or the flowing current (in TSC) are registered. The sample is then cooled down to the initial temperature T_0 . The sample is further heated to a higher temperature $T_2 > (T_1 + \Delta T)$ and then cooled down again. These heating/cooling cycles are implemented throughout the whole temperature range of the TSC or the TL bands. During the subsequent heating/cooling cycles, deeper and deeper traps are emptied, and the activation energy of the

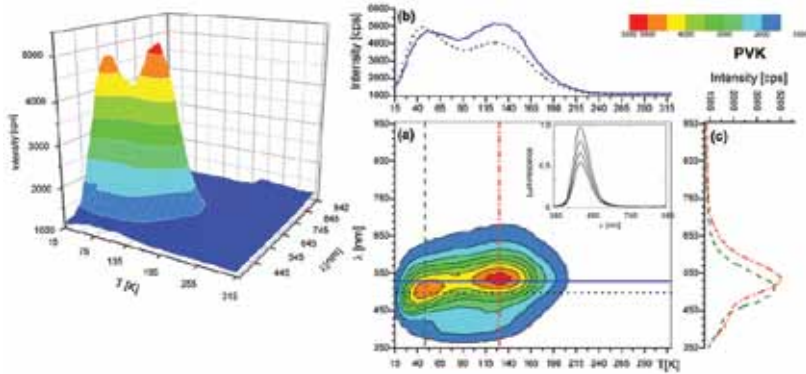


FIGURE 10

Three-dimensional TL spectra for the neat PVK films measured under a heating rate of 7 Kmin^{-1} after an excitation operated by a HBO-200 lamp with a band filter at 15K. The TL spectrum map for a neat PVK film (a) is presented with separated monochromatic TL curves (b) and spectrally resolved curves (c). The marked lines on the TL map indicate: the chosen wavelengths (horizontal lines) and the chosen temperatures (vertical lines). The inset presents the spectra of isothermal luminescence decay at 15K before the TL run [35]. © IOP Publishing. Reproduced with permission. All rights reserved.

consecutive detrapping process E_t could be calculated with the “initial rise method” proposed by Garlick and Gibson [34]. In this method, it is assumed that the initial rise of the TL or TSC maximum is described by:

$$I(T) = A \exp\left(\frac{E_t}{kT}\right) \quad (14)$$

where: I is the emitted light intensity (in TL) or current (in TSC), and A is a constant, related to the “attempt-to-escape frequency”. The expression in Equation 14 can only be applied if the temperature at which the sample is heated is low enough when compared to the maximum temperature T_{\max} , and if the number of electrons trapped remains constant and independent of the kinetics order. If a plot of $\ln(I)$ versus $1/T$ is drawn, then a straight slop line is obtained for the initial rise which follows the equation: $-\Delta E/k$. It follows that the activation energy for the detrapping of ΔE can be easily estimated. The calculated activation energies can then be plotted against the temperature range for which a given E_t value was obtained. Such a plot will reflect the distribution of the trap levels.

In the case of electroluminescent materials, especially with multicomponent systems, a very valuable information is the identification of active centres of radiative recombination. In the recent years, thanks to the “application of detection systems” based on CCD elements, the investigation of the trapping and the radiative recombination phenomena lead to the development of the spectrally resolved thermoluminescence (SRTL) technique [35].

This resulted in a three-dimensional (3D) graph allowing to track the changes in the emitted light intensity as a function of the temperature and the wavelength. From there, the TL curve could be separated for selected wavelength and the spectral distribution of the emitted light at a selected temperature could be determined (Fig. 10). This would enable to assess the contribution of the radiative recombination centres in the investigated material during the process of charge carriers release from the different types of traps. The spectrum analysis of the isothermal luminescence decay could also allow the evaluation of the participation of recombination centres in the relaxation of long-lived excited states.

2.2. Current–Voltage Characteristics

In the pure, undoped semiconducting polymers, the concentration of free charge carriers is very low, and the dependence of the steady-state space charge limited currents (SCLC) density j_{SCLC} on the applied voltage V for trap free semiconducting or insulating materials (assuming that the electrodes are ohmic and that there is no potential barrier for carrier injection) can be represented by the Mott–Gurney equation (the modified Child’s equation):

$$j_{SCLC} = \frac{9}{8} \frac{\epsilon \epsilon_0 q \mu V^2}{L^3} \quad (15)$$

where: q is the elementary charge, ϵ is the dielectric permittivity, ϵ_0 is the permittivity of the free space, μ is the charge carrier mobility, and L is the sample thickness [36, 37].

In materials with charge carriers traps the observed super ohmic behaviour at higher electric fields is related to the formation of space charge caused by free and trapped charge carriers. The theory of space charge limited currents elaborated for materials with shallow monoenergetic depth traps, E_t and density, N , predicts the dependence of the current density j_{SCLCT} on the temperature and on the electric field in the following form [36, 37]:

$$j_{SCLCT} = \frac{9N_{eff} \epsilon \epsilon_0 q \mu V^2}{8NL^3} \exp\left(\frac{E_t}{kT}\right) \quad (16)$$

where: N_{eff} is the effective density of states in the conduction band.

When shallow traps exhibit an energetic distribution, the dependence of the current density j_{SCLCT} on the electric field and on the sample thickness is the same as given in eq. (16), but the dependence on the trap concentration will be different [8].

Murgatroyd demonstrated that when the traps are charged—when—empty, the Poole–Frenkel effect would lead to a stronger dependence of the current density j_{SCLCT} on the applied voltage than that predicted by eq. (16) [38]. Such a strong dependence of the current on the applied voltage was found by Helfrich and Mark in thin single crystals of diphenyl, *p*-terphenyl, *p*-quaterphenyl, naphthalene and anthracene [39].

A more detailed analysis of the charge carrier transport and trapping phenomena in semiconducting polymers was performed by Blom and coworkers [4] on the basis of the current–voltage characteristics in the single–carrier devices. Remarkably, a different holes and electrons transport mechanisms were identified. The hole conduction, in most of the semiconducting polymers, can usually be well described by the trap–free SCLC model. Furthermore, the dependence of the mobility on the electric field and on the charge–carrier density appears typical for the hopping mechanism in materials with density of states following a Gaussian distribution [40, 41]. The electron current is, in contrast, controlled by the trap–limited–conduction (TLC) mechanism and characteristic feature of the electron conduction is strong dependence on the voltage and on the sample thickness. The modelling of the I – V characteristics indicated that the electron trap states in semiconducting polymers exhibit a Gaussian distribution inside of the band gap [4, 42]. The modelling of the temperature–dependent TLC for electrons, for a series of semiconducting polymers was performed with an assumption, that intrinsic electron mobility in semiconducting polymers is similar to the hole mobility, and the intrinsic hole mobility was obtained from measurements of the hole–only diodes [4]. It was then possible to determine the width of the Gaussian density of states distribution of the HOMO and the LUMO; it was assumed that width of the Gaussian trap distribution is the same which sounds like a reasonable assumption taking into account that these distributions result from the same disorder. It follows that with such assumptions, the modelling of the temperature dependent electron TLC enables to assess the electron trap density N_t and trap depth E_t . It was then unexpectedly found that for all investigated polymers the density of the electron traps is very similar, around 3×10^{23} traps per m^3 . Moreover, for all these polymers the trap distribution was similar and was located at similar energy, ca 3.6 eV, below the vacuum level. This could be explained by the common origin of the electron traps in semiconducting polymers, bis–hydrated–oxygen complexes. This conclusion was also supported by quantum chemical calculations. The electron trap depth in a given polymer is determined by the position of LUMO level. This would explain why in polymers with higher LUMO levels the current displays a stronger dependence on the voltage. It results from the fact that deeper traps lead to steeper I – V characteristic. It is important to underline that the value of trap depth (ca. 0.7 eV) determined from the I – V modelling for poly(*p*-phenylene vinylene) is close to

trap depth of ca. 0.75 eV obtained from the photocurrent measurements and the photo-thermal deflection spectroscopy [21].

2.3. OFETs modelling

The unified model and parameter extraction method (UMEM model) provides a rigorous and accurate method for the determination of the main electrical parameters of organic field effect transistors [43]. The density of traps cannot be directly extracted from the UMEM model. It has however been shown that the density of traps could be estimated from the dependence of the charge carriers mobility μ_{FET} on the drain-source voltage V_{DS} , with a set value of the gate-source voltage V_{GS} . An increase of mobility could be related to the Frenkel-Poole effect (i.e. field enhanced thermal excitation of the trapped charge carriers) [44].

Another approach considers that for gate-source voltages in the sub-threshold region the density of trap states at the semiconductor/dielectric interface N_{it} can be calculated from the subthreshold swing SS (equation (12)) [45]:

$$SS = \frac{kT}{q} (\ln(10)) \left(1 + \frac{q^2 N_{it}}{C_{di}} \right) \quad (17)$$

where C_{di} is the dielectric capacitance.

Mao *et al.* [46] have calculated the density of traps using the parameter SS in OFETs based on vacuum deposited pentacene. They determined that the interface trap densities were in the range of 10^{11} to 10^{12} cm⁻² eV⁻¹. It is important to mention that these values are several orders of magnitude higher than the interface trap density in silicon-based field-effect transistors.

3. EXAMPLES OF EXPERIMENTAL RESULTS RELATED TO CHARGE-CARRIER TRAPPING

3.1. Organic Light Emitting Diodes

The efficiency of polymer light-emitting diodes is generally connected to the charge transport and the charge recombination processes [6, 7], both of which can be strongly influenced by the trapping phenomenon. Many different approaches and techniques have been applied to strengthen the knowledge around this issue. In this part we will introduce selected examples of applications of the TL technique in order to investigate the trapping in electroluminescent materials (including both electroluminescent conjugated polymers and host-guest systems, in which low molecular weight emitters are dispersed in polymer matrices).

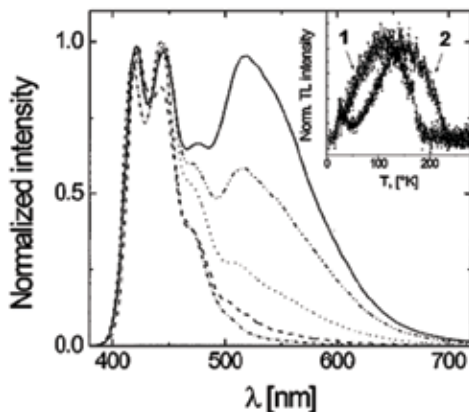


FIGURE 11

EL spectra of different layers: PF C26 (—), PF C26+TPTE(---), PF C26+ST 16/7 (.....), PF C26+ST 755 (-.-.-). The photoluminescence spectrum of PF C26 is also presented (-.-.-). The inset shows the normalized thermoluminescence (TL) glow curves of pure PF C26 (curve 1) and a blend with 3 wt % TPTE (curve 2). Reprinted from [48], with permission of AIP Publishing.

One of the most intensively investigated electroluminescent polymers are the polyfluorenes, which are characterized by an efficient emission of blue light. However, an undesirable green emission was also observed in the electroluminescence spectrum [7]. The formation of aggregates, of excimers or of keto defects were proposed as possible explanations for this effect [47]. On the basis of the TL studies it was found, that an addition of a small amount of nonradiative molecules, whose HOMO level is located above the HOMO level of polyfluorenes, causes the formation of new, deeper hole traps, which prevent the capture of charge carriers by the ‘green-emitting sites’. This results in both the quenching of the undesirable low-energy emission and the increase of the electroluminescence (EL) efficiency [48, 49]. The EL spectra of poly(2,7-(9,9-bis(2-ethylhexyl)co-(9,9-bis((3S)-3,7-dimethyloctyl)) fluorene) (PF C26) doped with different triphenylamine derivatives (TPTE, ST 16/7, ST 755) are shown in Fig. 11. Upon the addition of one of them, i.e. N,N'-diphenyl-N,N'-bis(di(3-methyl-phenyl)-amino-biphenyl)-benzidine (TPTE), the green emission (above 500 nm in the EL spectrum) is almost completely suppressed. The TL spectra indicate that the addition of TPTE to the PF C26 results in the formation of deep trapping levels. This manifests itself by a shift of the TL maximum to higher temperatures of around 50 K (Fig. 11, inset) [48].

Additionally, the trapped holes create a space charge field, which enhances the electric field at the cathode and facilitates the injection of electrons. This leads to an improvement of the electron/hole balance. This interpretation is supported by the luminance-versus current density dependence of the devices (Fig. 12, inset). In all of the cases, the addition of the triphenylamine derivatives enhances the luminous efficiency when compared to the pure PF C26 devices.

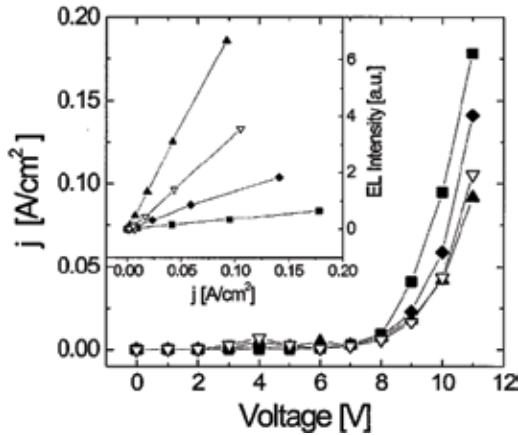


FIGURE 12

Current–voltage characteristics of OLEDs based on polyfluorene and its blends: pure PF C26 (■), PF C26+TPTE (▲), PF C26+ST 755 (◆), and PF C26+ST 16/7 (▽), at a concentration of HTM of 3 wt %. The inset shows the luminance vs the current characteristics. Reprinted from [48], with permission of AIP Publishing.

Similar trapping effects were observed for poly(9,9-bis(2-ethylhexyl)fluorene) (PF2/6) doped with TPTE [49] or with tri-*p*-tolylamine (TTA) [50].

The triphenylamine derivatives (TPA) which are connected to the fluorene chain by chemical bonding modify the electroluminescence performance of the polyfluorene by inducing a similar effect, i.e. introducing deep trapping centres [51]. For copolymers, with TPA attached as pendant groups (PFco1, PFco2), a new high-temperature band in the TL spectra with a maximum at about 150 K appears (see Fig. 13a).

Its relative intensity increases with the increasing content of TPA, which is higher in PFco2 than in PFco1. Thanks to the results of the partial heating experiment, the presence of deep traps (above 200 meV) located on TPA groups were identified (Fig. 13b). However, for the polyfluorene with TPA molecules attached to each of the monomer unit, there was no observable TL band (see the TL curve for the PFhomo2 in Fig. 13a). This could be because the TPA derivatives are hole transport materials and when their density in the polyfluorene chain is high, they form new transport paths rather than hole traps. The long-wavelength emission band originating from the “green-emitting” sites was also eliminated in the chemically modified polyfluorenes [51].

An important class of polymer light emitting diodes (PLEDs) consist of the systems with a host-guest emission layer made of a polymer matrix and a low molecular weight emitter. A commonly used host matrix is made of a mixture of poly(*N*-vinylcarbazole) (PVK) and of 2-(4-*tert*-butylphenyl)-5-(4-biphenyl)-1,3,4-oxadiazole (PBD). The trapping phenomenon in the PVK and the PVK-PBD blends were also investigated by means of the TL technique [35, 52].

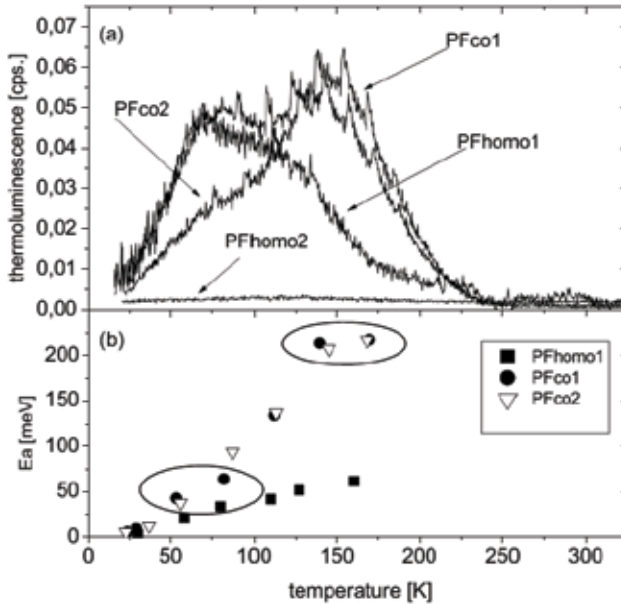


FIGURE 13

The TL spectra (a) and the activation energy obtained from the partial heating (b) for the investigated neat polyfluorene homopolymer PFhomo1, and for the polyfluorenes chemically modified with TPA derivatives: copolymers PFco1 and PFco2 and homopolymer PFhomo2. The spectra are non-normalized. Reprinted from [51], with permission from C. Galotiotis—legally responsible for the J. Nanostruct. Polm. Nanocomp.

The TL partial heating experiments for neat PVK revealed the presence of two main trapping levels: one around 50 meV and one around 200 meV, which related to the low and high-temperature TL maxima, respectively (the TL results for PVK are shown in Fig. 10).

The addition of 40 wt% PBD to the PVK resulted in a considerable change in the TL spectrum, as presented in Fig. 14 [35]. The monochromatic TL curve for a wavelength $\lambda = 550$ nm (Figure 14(b)) has a maximum at 105 K and a shoulder in the low-temperature range, which relates to the low-temperature maximum observed for neat PVK (Fig. 10). A shift of the position of the main TL peak from 130 K for neat PVK to 105 K for the PVK–PBD blend indicated that in the blend, shallower traps dominate, with a depth of about 150 meV as determined by the partial heating experiments [35].

The average value of the activation energy for the carriers release at a temperature corresponding to the TL maximum is proportional to the so-called parameter of “effective disorder energy”. On the basis of the TL results, the effective width of the density of states (DOS) distribution and the average energy of the charge carriers in relation to the centre of DOS distribution can be determined [53–55]. The obtained values were consi-

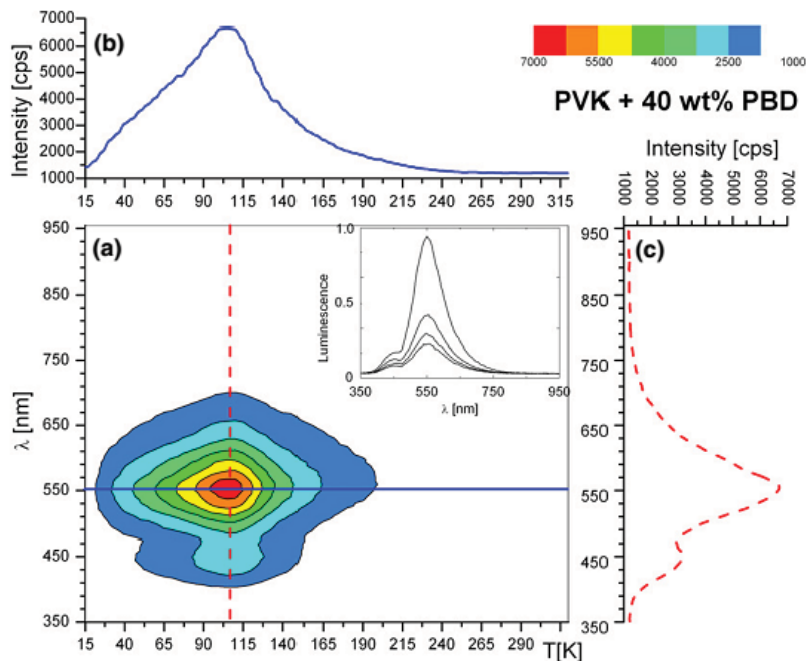


FIGURE 14

TL spectrum map for the PVK-PBD (40 wt%) blend film (a) with a separated monochromatic TL curve (b) and a spectrally resolved curve (c). The marked lines on the TL map indicate the chosen wavelength (horizontal line) and the chosen temperature (vertical line). The inset shows the spectra of the isothermal luminescence decay at 15K before the TL run [35]. © IOP Publishing. Reproduced with permission. All rights reserved.

tent with the results obtained from the time of flight experiment for PVK [56, 30].

The comparison of the EL and SRTL spectra for the PVK and PVK-PBD systems (see Fig. 15) indicated that different radiative recombination centres were dominant in the electroluminescence and in the thermoluminescence.

For the EL spectra, the band associated with the singlet excimer states (at 400 nm) dominated, however, a long wavelength emission in the 470 – 600 nm range was also identified which could mainly be attributed to the triplet excimer states.

The addition of PBD to PVK reduced slightly the EL emission in the range of 470 nm and of 600 nm. This was due to the lower concentration of carbazole groups in the mixture and to the formation of triplet PVK/PBD exciplexes which compete with the creation of triplet PVK excimers. On the other hand, in the SRTL spectra dominate the long-wavelength emission from triplet excimer or triplet exciplex clearly for the neat PVK and the PVK/PBD blend, respectively [35].

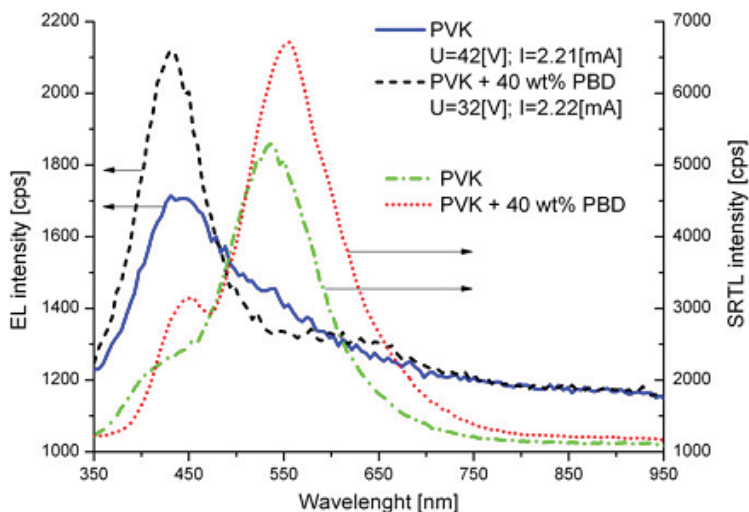


FIGURE 15

Comparison of the EL spectra of a single layer PLEDs and of the SRTL spectra registered at the TL maximum temperature for both PVK and PVK–PBD (40 wt%) films (extracted from figure 10(c) and from figure 14(c)) [35]. © IOP Publishing. Reproduced with permission. All rights reserved.

The PVK and PVK–PBD blends are particularly useful, acting as host matrices for the phosphorescent guest molecules because of the PVK high triplet exciton energy that prevents the crossing of the triplet guest exciton back to the host triplet state [35, 52]. These interesting results provided TL studies for the PVK and the PVK + 40 wt% PBD doped with 1 wt% fac–tris(2–phenylpyridine) iridium (III) ($\text{Ir}(\text{ppy})_3$) [57].

As presented in Fig. 16, the presence of a 1 wt% complex causes the low–temperature TL maximum to disappear, and a new, high–temperature band is observed. This one is particularly visible when the PVK is doped with 1 wt% $\text{Ir}(\text{ppy})_3$. Partial heating experiments are shown in Fig. 16(b) indicated that this TL maximum is related to deep (350 – 400 meV) hole traps. This value is close to the difference between the HOMO levels in PVK and in $\text{Ir}(\text{ppy})_3$, (5.8 and 5.4 eV, respectively).

However, it should be emphasised, that the energy of the HOMO/LUMO levels of molecules is not only dependent on the chemical structure but also on the surrounding electronic polarisation which is particularly important in the host–guest systems. It was found that the presence of highly polar emitter molecules (dipole moment of approximately 6 D) [58] will affect the activation energy relating to the release of charge carriers trapped in the matrix. The interaction between the charge carriers and the randomly oriented dipoles of the emitter molecules will cause the energy of some states of the PVK/PBD (located close to the emitter) to be lowered (see Fig. 4 and the inset in Fig. 16). A similar effect of shifting of the TL maximum to

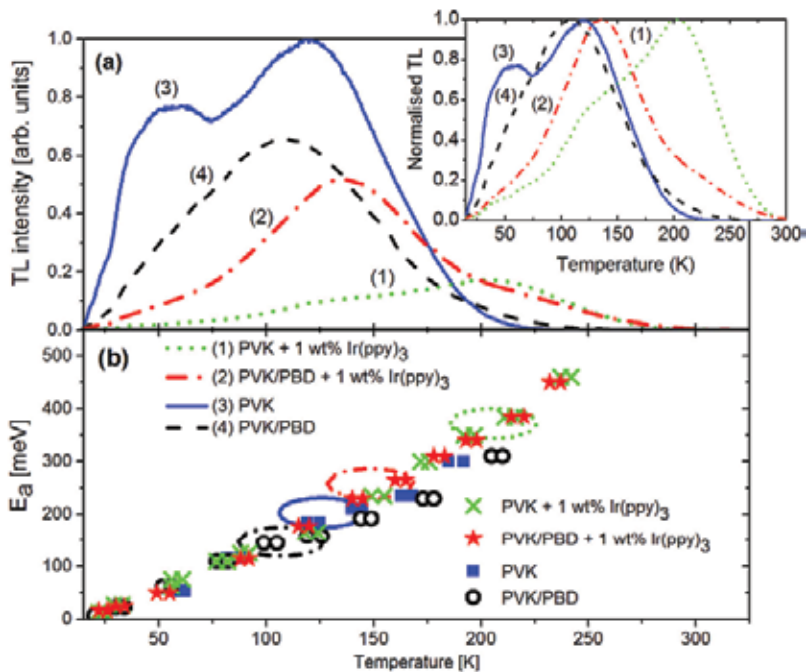


FIGURE 16

TL spectra (a) and activation energy obtained from the partial-heating experiments (b) for PVK and PVK/PBD doped with 1 wt% Ir(ppy)₃. For the purpose of comparison, the TL curves and the results of the partial heating experiments for neat PVK and PVK/PBD are added. The marked ellipses indicate the presence of dominating trapping levels corresponding to the TL maxima. The (a) inset presents the normalised TL glow curves of the investigated systems. Reprinted from [57], with permission from Elsevier.

higher temperatures after the introduction of polar molecules to the polymer matrix (poly(N-epoxypropylcarbazole)) was described by Kadashchuk *et al.* [59].

The TL technique usually applied for the characterisation of the trapping phenomena can also be used in combination with an on-line spectral analysis of the emitted light (SRTL), which can help in identifying the radiative recombination mechanisms in the host-guest emissive layers. An example of the SRTL results for PVK doped with red emitting bis[2-2'-benzothienyl]pyridinato-N,C³⁺](acetylacetonate) iridium (Ir(btp)₂(acac)) is shown in Fig. 17 [60].

It is apparent that the addition of the Ir(btp)₂(acac) molecules to PVK drastically affects the spectrum of the light emitted in the course of the TL experiment. A dominant emission maximum occurs at about 630 nm and its position is not influenced by temperature. At this wavelength, the monochromatic TL curve is dominated by a broad band at a maximum of about 200 K. The shape of the monochromatic curve is similar to the one of the

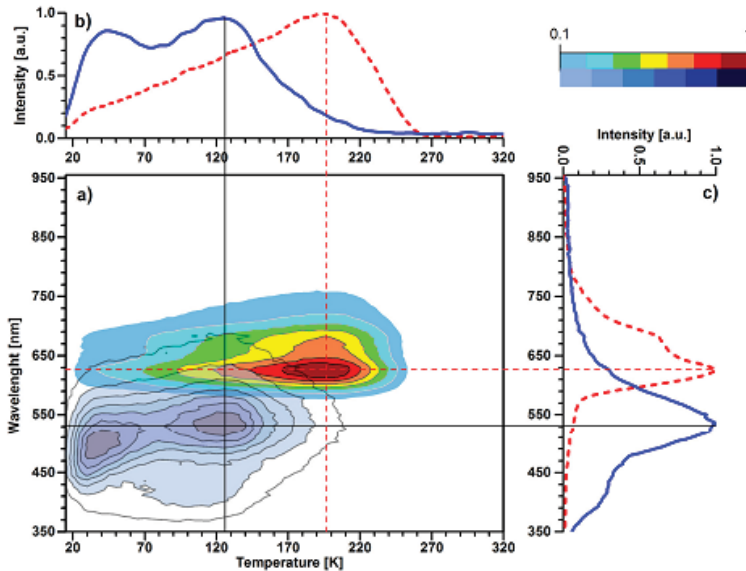


FIGURE 17

SRTL spectrum map for a PVK + 1 wt% Ir(btp)₂(acac) film (a); monochromatic TL curve registered at $\lambda = 630$ nm (b); spectral resolved curve registered at ca. 200 K (c). For the purpose of comparison, the analogous SRTL results for undoped PVK are also displayed. Reprinted from [60], with permission from Elsevier.

TL curve for PVK doped with Ir(ppy)₃ (see curve 1 in the inset of Fig. 16). This indicates that in this case, besides the presence of trap states on the PVK matrix (with a depth ranging from tens of meV to 200 meV), the main formed traps are deeply located on the Ir(btp)₂(acac) molecules. The comparison of the position of the HOMO levels in PVK (5.8 eV) and in Ir(btp)₂(acac) (5.2 eV) suggests that in this system hole traps with a depth of 0.6 eV may be formed. A similar value for the activation energy (i.e. 0.55 eV) corresponding to the TL peak at 220 K was obtained by Kadashchuk *et al.* for Ir(btp)₂(acac) doped into poly[1,4-bis(6'-cyano-6'-methylheptyloxy) phenylene] (CNPPP) [61].

The SRL spectrum recorded at 200 K relates to the triplet excitons of the Ir(btp)₂(acac) molecules. This emission is different from that registered close to the TL maximum (at 125 K) of the undoped PVK (see Fig. 17c). It then follows that the process of charge carriers release from all traps results only from the emission of the red emitter molecules. Single layer PLEDs based on the investigated system (PVK doped with 1 wt% Ir(btp)₂(acac)) were prepared to check what kind of radiative recombination centres operate during the electrical excitation. Fig. 18 presents the EL spectra of two devices: one based on PVK doped with the iridium complex for various bias voltages and the second based on an undoped PVK emissive layer. The PVK emission is almost completely quenched upon doping with 1 wt%

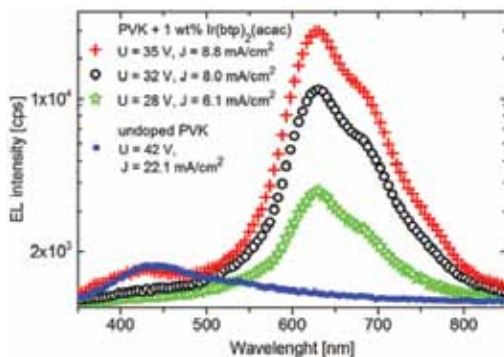


FIGURE 18

Electroluminescence spectra of a single layer PLED with PVK doped with 1 wt% Ir(btp)₂(acac) as an emission layer. The spectra were recorded at various bias voltages. The EL spectrum of the PLED based on undoped PVK is also shown for comparison. Reprinted from [60], with permission from Elsevier.

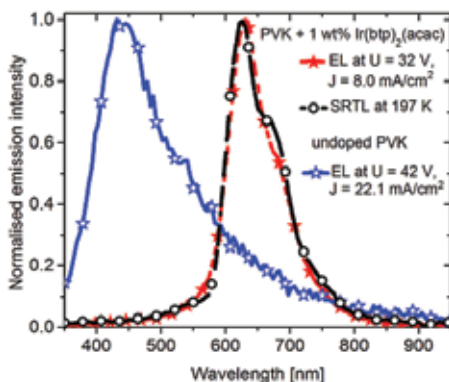


FIGURE 19

Comparison of the normalised spectra of PVK doped with 1 wt% Ir(btp)₂(acac): EL is measured at room temperature and SRTL at ca. 200 K. Additionally the EL spectrum of the neat PVK at room temperature is presented. Reprinted from [60], with permission from Elsevier.

Ir(btp)₂(acac), and the emission is related to the triplet excitons of the iridium complex molecules.

In order to directly compare the spectra obtained with the optical and electrical excitation, the normalised EL and SRTL spectra for PVK doped with 1 wt% Ir(btp)₂(acac) are presented in Fig. 19. Considering that the spectral distribution of the emitted light recorded during the TL experiment and the light emitted by the PLEDs are identical, one can conclude that the mechanism of radiative recombination is the same for both types of excitations. This effect can be explained as follows: in the electroluminescence phenomenon, the charge carriers are continuously provided from the electrodes and travel to the emissive layer. They are then captured by the localised states on the PVK and by the emitter molecules (in a similar way as in the TL experiment).

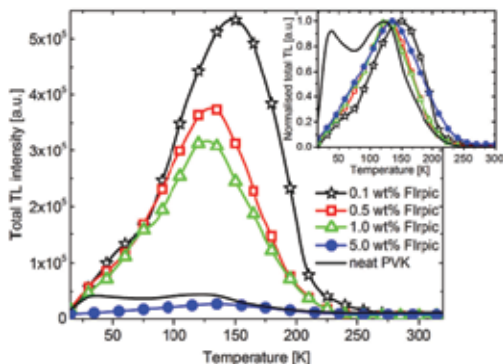


FIGURE 20

Total TL intensity as a function of the temperature (TL spectra) for neat PVK and PVK doped with 0.1, 0.5, 1.0 and 5.0 wt% FIrpic. Inset: same TL spectra after normalisation. Reprinted from [62], with permission from Elsevier.

However, since the electroluminescence experiment is carried out at room temperature, the charge carriers are promptly released from these traps and they recombine radiatively, obeying the same mechanism as the one presented for the TL experiments.

The described mechanisms for the generation of excitons on the emitter molecules in the PVK doped with iridium complexes were confirmed by the SRTL experiments [62] for the systems with two iridium complexes emitting a blue–green light: bis(4,6–difluorophenyl) pyridinato–N,C^{2'}) (picolate) iridium (FIrpic) [63] and tri(2–(2,4–difluorophenyl) pyridine) iridium (Ir(Fppy)₃) [64]. The location of the HOMO and the LUMO levels of the iridium complexes relative to the levels of PVK indicated that the emitter molecules embedded in the matrix would not create traps for the holes (such was the case for the Ir(ppy)₃ and the Ir(btp)₂(acac)). It could however form deep electron traps (with a depth of 0.7 eV).

The impact of the doping level of PVK on the trapping and on the radiative recombination processes was also studied and the TL results are presented in Fig. 20. An addition of merely 0.1 wt% FIrpic to the PVK caused a substantial reduction of the low–temperature TL band (presenting with a maximum at about 50 K). In the meantime, the total intensity of the TL increased by ca 1 order of magnitude when compare to pure PVK. The calculations indicated that for 0.1 wt% FIrpic the concentration of deep electron traps is about $1 \times 10^{17} \text{ cm}^{-3}$, which is close to the estimated concentration of hole traps in a PVK matrix. However, a further increase of the FIrpic content would result in a reduction of the total TL intensity, due to the concentration quenching effect and the triplet–triplet annihilation of the emitter molecules.

The spectral distribution of the emitted light at temperatures corresponding to the TL maximum showed that the emission occurs in the same range as

the characteristic bands coming from the triplet states of FIrpic (regardless of the dopant content) [62].

3.2. Organic Photovoltaic Devices

The current flowing in the photovoltaic device (I) is the sum of the diode dark current and the photocurrent I_{ph} . The current vs voltage (I - V) characteristics of the organic semiconductor heterojunctions are often analysed in a similar way as inorganic p - n junctions, by means of a theoretical approach based on the generalized Shockley equation:

$$I = I_s \left[\exp\left(\frac{qV}{nkT}\right) - 1 \right] - I_{ph} \quad (18)$$

where I_s is the reverse bias saturation current, V is the applied voltage and n is the ideality factor related to the mechanisms of charge carrier transport and recombination. For an efficient photovoltaic device this last parameter should be comprised between 1.3 and 1.8. Higher n values would induce a decrease in the photovoltaic efficiency.

Even though organic and inorganic semiconductors present fundamental differences in their physical mechanisms, in several cases the inorganic approach offer a good reproductive description of the performance of Organic Photovoltaic (OPV) devices. However, in inorganic solar cells, consisting of semiconductors with classical energy bands, the excitons dissociate readily into free charge carriers, while in organic semiconductors, the excitons energy of dissociation is much higher. The transport of the generated charge carriers is also governed by the hopping mechanism and the charge carrier mobility is affected by numerous localized and trapping sites.

3.2.1. Trap-limited recombination

In practice, in every OPVs and in particular in BHJ systems, the active layers, made of donor and acceptor semiconductors, are strongly disordered. Consequently, the distribution of the density of states (DOS) at both HOMO and LUMO levels would be very broad. The DOS in disordered organic semiconductors is usually described by the Gaussian distribution [65]. However, the low-energy tail of the DOS can remarkably be approximated by the exponential distribution. Most of the charge carriers occupy the lower energy part of the DOS, and the low-energy tail states could therefore be treated as traps [66].

The DOS at the p - n interface appears to be additionally broadened due to the donor-acceptor interactions. This is affecting the kinetics of the recombination in BHJ at the p - n interface, as illustrated in Fig. 5(b) (Sec. 1.3): in there, the photogenerated electrons (e) recombine with the positively charged traps (p_T) localised in the donor phase (close to the interface). Similarly, the photo-

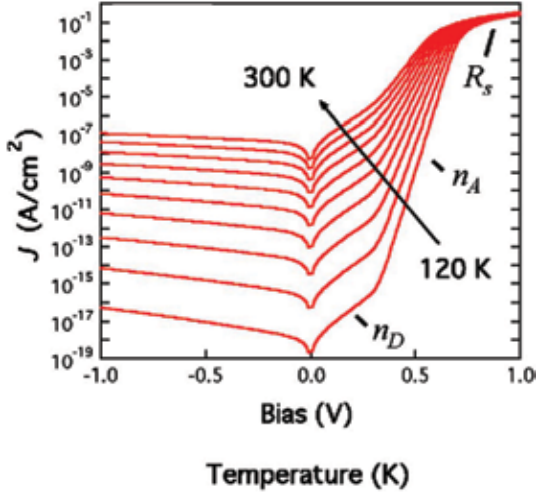


FIGURE 21

Double exponential dark current. The voltage characteristics are calculated according to Eq. 19. Reprinted Figure with permission from [66]. Copyright (2017) by the American Physical Society.

generated holes (h) recombine with negatively charged traps (n_T) localised in the acceptor phase (close to the interface). It follows that the ideality factor n in the diode equation (18) may increase [67]. Moreover, when the density of the trapped charge carriers becomes higher than the density of free charge carriers, the recombination at the p - n interface yields a two-exponential diode equation, with two temperature dependent ideality factors $n_A(T_A)$ and $n_D(T_D)$:

$$I = I_{sD} \left[\exp \left(\frac{qV}{n_A(T_A)kT} \right) - 1 \right] + I_{sA} \left[\exp \left(\frac{qV}{n_D(T_D)kT} \right) - 1 \right] - I_{ph} \quad (19)$$

where I_{sA} and I_{sD} are the electron and the hole saturation currents, respectively. These two currents are dependent on the density of trap states at the acceptor and donor phases. They also depend on the characteristic electron and hole traps temperatures T_A and T_D respectively.

In the dark current-voltage characteristics, specifically in the 120 K to 300 K temperature range (see Fig. 21), one can recognize in the forward (positive) bias direction, three regions with dominating different mechanisms. The first one is below 0.3 V and is characterised by a trap-limited recombination of the free acceptor electrons and the trapped donor holes. Here, the characteristic slope is proportional to the donor ideality factor n_D . The second one ranges from 0.3 V to 0.8 V and is characterised by the recombination of free donor holes with trapped electrons acceptor. In there,

the slope is proportional to the acceptor ideality factor n_A . Finally, the third one, at higher voltages the current is limited by the contacts and the bulk resistance R_s .

A double exponential characteristic can also be observed in inorganic p - n junctions. Two ideality factors are often found if the recombination is governed by two different mechanisms; in both inorganic and organic amorphous systems. This is due to the broad distribution of the trapping sites resulting from the disorder [66, 67].

3.2.2. Role of impurities

In the OPVs based on BHJs, which were made of high purity semiconductors, the efficiency of the photovoltaic effect can be determined to a great extent by the Langevin-type bimolecular recombination [68]. Such a recombination is described by a 2nd order kinetic, and if the density of the photogenerated electrons and holes is high, then the probability of bimolecular recombination would also be relatively high. The recombination influences the charge carrier separation and transport, and therefore affects all the basic parameters of the OPVs: the short-circuit current density J_{SC} , the open-circuit voltage V_{OC} , the fill factor FF and the power conversion efficiency PCE (Fig. 6 in Sec. 1.3). However, in most of the OPV devices the traps resulting from impurities and defects are inevitable. Moreover, when their amount exceeds a critical concentration, the OPV characteristics will considerably deteriorate. Furthermore, when the free charge carriers are captured by charged traps, the kinetics order of the trap-assisted recombination decreases [68].

Cowan *et al.* [69] have performed investigations on the photovoltaic effect in the OPVs with a controlled density of traps. A copolymer, the poly[N-9"-hepta-decanyl-2,7-carbazole-alt-5,5-(4',7'-di-2-thienyl-2',1'3'-benzothiadiazole) (PCDTBT) was chosen as a model system and mixed with [6,6]-phenyl C₆₁ butyric acid methyl ester (PC₆₀BM) at a very high purity. [6,6]-phenyl C₈₄ butyric acid methyl ester (PC₈₄BM) molecules were introduced in such a nearly trap-free system as potential electron traps. These molecules act as traps since the LUMO level of PC₈₄BM is 0.35 eV, which is lower than the LUMO of the PC₆₀BM (4.3 eV). A reduction in the short circuit current, I_{SC} , and in the fill factor, FF , was identified at very low concentration of PC₈₄BM, with weight ratio PC₈₄BM:PC₆₀BM = 1:1000. Moreover, for a ratio of 1:10, a dramatic deterioration in the OPV performance was observed, which was due to the enhanced recombination loss.

Interestingly, the steady-state dark current density vs. voltage characteristics measured in BHJ solar cell devices with small amounts of PC₈₄BM traps presented a similar shape as the double-exponential characteristics shown in Fig. 21. Then, based on the Shockley, Read, and Hall recombination model [70, 71] a decrease of the open circuit voltage V_{OC} with the

increase of the concentration of PC₈₄BM could be attributed to the increase of the trap-assisted recombination. It was concluded, that the ratio between the trap-assisted recombination rate and the photogeneration rate determines the transition from the bimolecular to the trap-assisted recombination regimes. For BHJs with a low trap density and under high light intensities, the open circuit voltage V_{OC} is not significantly reduced by the trap-assisted recombination. However, in many cases, the presence of (usually inevitable) traps leads to the decrease of the V_{OC} [69].

3.2.3. Fermi-level shift

It is generally accepted, that the open-circuit voltage V_{OC} in heterojunctions OPVs is related to the difference between the HOMO level of the donor and the LUMO level of the acceptor components. It should however be emphasised that the HOMO and LUMO levels (obtained with cyclic voltammetry measurements) are to be treated with a great caution for application to real BHJ [72]. Indeed, the perturbation of the HOMO and the LUMO levels, caused by the energy disorder and the donor-acceptor interactions at the interface, would determine the open-circuit voltage [73].

Also, even though the traps density, generated by the impurities left from the synthesis or by the processing procedures, would be very low, some charge carriers will occupy the states in the low-energy tail of the DOS. Hence, these states will act as effective traps [66]. The accumulation of charges in such localized states at the donor/acceptor interface of BHJ systems will influence the Fermi levels for the holes in the donor phase and for the electrons in the acceptor phase. A broad distribution of the density of states, typical for organic BHJs, will therefore result in different electron statistics when compared to crystalline inorganic semiconductors. It will also constrains the V_{OC} values. It was indeed demonstrated, that for BHJ solar cells with the same donor (P3HT) but with two different fullerene acceptors with a higher and a lower number density of states, a higher open-circuit voltage appeared for fullerene with the higher DOS [74].

3.3. Organic Thin Films Transistors

Origins of the charge carriers trapping sites in the OTFT

The most important parameter in the characterization of the performance of OTFTs is the charge carrier mobility μ_{FET} . As introduced before, the transport in transistors occurs in a very thin semiconductor layer, adjacent to the gate dielectric, in which the charge carrier density is modulated by the gate voltage. For a low charge carrier density, the charges are immobilized in traps, energetically far away from the transport states. However, with an increasing gate voltage the traps are gradually filled and more and more charge carriers are moved to transport states. Therefore, in a high traps density case, the charge carrier mobility would be determined from the current-voltage characteristics (see Introduction) and would be dependent on the gate voltage [75]. Interestingly,

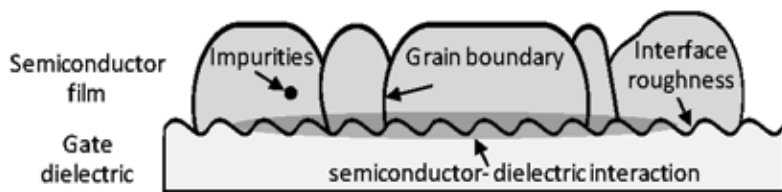


FIGURE 22

Schematic cross-section of the semiconductor and the insulator layers. The places with the most recurrent charge carrier trapping are indicated.

when traps are inhomogeneously distributed, presenting a higher density at the dielectric interface, the determined mobility could decrease with an increasing charge carrier density (i.e. with increasing gate voltage) [76].

The presence of traps in organic semiconductors is inevitable. An energetic and positional disorder would result in a broad distribution of the density of states, with a tail comprising deep lying localized states. The structural and morphological defects are sources of traps at the grain boundaries. Other hole or electron trap sources include: the impurities and the dopants. This strongly depends on their ionization potential and their electron affinity in relation to the host material. Aside from the traps, there are localized states in the semiconducting layers of OTFTs which are created at the interface with the gate dielectric (see Fig. 22).

3.3.1. Molecular disorder

The highest values for the charge carrier mobility were reported for OFETs with single crystals or with an ordered polycrystalline structure. This could strongly be attributed to the overlapped π - π orbitals that facilitate the charge transfer between the molecules. This is contrasted with the random distribution of molecules hindering the transport [77, 78]. Dimitrakopoulos provided such a demonstration [79], with the description of a series of OTFTs with pentacene layers with different level of molecular order. It was found, that the charge carrier mobility increased from 10^{-9} cm²/Vs to 0.6 cm²/Vs with the increase of the molecular order.

The importance of the long-range molecular order was also demonstrated through the use of a zone-casting technique, in order to fabricate OTFTs with highly ordered layers of organic semiconductors, both *p*- [80] and *n*-type [81]. The transistors with semiconducting layers obtained by zone-casting exhibited a much higher mobility than the one made of the same, but disordered semiconductors.

3.3.2. Grain boundaries

The borders between the crystalline regions act as traps for charge carriers. This happens in both the polycrystalline low molecular weight semiconductors and the partly crystalline conjugated polymers [82]. In the last one spe-

cifically, the transport of charge carriers takes preferably place within the lamellas. The crucial role of the nanofibrils on the charge carrier transport in the ultrathin layers of the regioregular poly (3-hexylthiophene) (P3HT) was recently demonstrated by Janasz *et al.* [83]. It was found, that the P3HT nanofibrils, obtained from an aged solution, yield an efficient conducting network, even with ultrathin films. Thanks to the formation of long nanofibrils, with a pronounced internal crystallinity and a long π -stacking coherence length, the hole mobility in an OTFT with a 8 nm thick layer of P3HT was as high as $0.1 \text{ cm}^2/\text{Vs}$. This demonstrated that by adjusting the morphology of the ultrathin semiconducting layer properly, one can reduce the effect of both the intergrain barriers and the traps, on the charge carrier mobility.

Semiconductor–dielectric interface

The performance of the OTFTs is often deteriorated by the charge carrier traps existing at the semiconductor/dielectric interface. The origin of the traps can be very different: the adsorbed impurities at the dielectric surface (mainly water, oxygen and hydrated oxygen complexes) [84, 85], the interface dipoles [86], the electronic polarization for high- k dielectrics or the roughness of the dielectric surface [87]. All these factors may induce a structural and energetic disorder in the semiconductor layer adjacent to the dielectric surface.

Impurities at the semiconductor/dielectric interface

Water, oxygen, hydrated oxygen complexes or other molecules adsorbed at the dielectric surface, can form trapping states which would result in the reduction of the drain current I_{DS} flowing into the transistor channel. This would similarly influence the dependence between the evaluated charge carrier mobility and gate voltage V_{GS} [85]. Furthermore, the accumulated and immobilised charge carriers at the interface are responsible for the shift of the threshold voltage V_{th} . Interestingly, the charge carriers migrate slowly into the dielectric bulk when the transistor remains polarised for a long time under an applied V_{GS} and/or V_{DS} voltage, which induce a change of V_{th} . This is known as the bias–stress effect [88]. Mathijssen *et al.* [89] have demonstrated that the trapped charges, which cause a shift in the threshold, are located at the dielectric gate and not in the semiconductor.

In the most of the reported studies on OTFTs, the substrates are doped Si wafers with chemically or thermally produced SiO_2 layers (of usually 200–400 nm thick). This play the role of the gate dielectric. It is well known, that any SiO_2 surface presents a high density of silanol groups, which efficiently create electron traps. It is therefore a common procedure to neutralize these traps by depositing self-assembled monolayers such as hexamethyldisilazane (HMDS), alkanetrichlorosilanes, or alkanephosphonic acids, on the SiO_2 surface [17].

In contrast, other often used dielectrics, such as parylenes (xylylene polymers) for example, are recognized for their high degree of purity. They are the produce

of a polymerization method which does not require the use of an external initiator. It is initiated by a monomer molecule which is in its excited diradical state [90]. Consequently, these dielectrics involve a relatively low number of localized states on the dielectric/semiconductor interfaces. The differences between the SiO₂ and parylene dielectrics were presented by Pfattner *et al.* [91]. They found that transistors made of single crystal of dithiophene-tetrathiafulvalene with parylene dielectric exhibit a higher charge carrier mobility than the transistors with the same single crystal but including SiO₂ dielectric. Interestingly, for the transistor with the parylene dielectric, there was almost no observed hysteresis in the current-voltage characteristics. This indicated a low density of traps and therefore a high quality interface between the organic single crystal and the dielectric.

In this context, it is interesting to refer to Wang *et al.* [92] work. They demonstrated that one can artificially introduce traps at the semiconductor/parylene interface by using an oxygen plasma treatment on the parylene. This was proven to considerably deteriorate the transistor performance. The charges fixed in the traps at the surface were consequently responsible for the observed V_{th} shift. The plasma would break the parylene bonds at the surface, resulting in the creation of mobile charges, which in turns increase the bulk conductivity of the dielectric. The consequence would be an increase of the parasitic I_{OFF} current.

Interactions with the gate dielectric-interface dipoles

To reduce the gate voltage required for operating of OTFTs, one can either reduce the thickness of the gate dielectric, or use a dielectric material with a high permittivity ($k > 4$). Both solutions however have serious drawbacks: the decrease of the dielectric layer thickness, the increase of the parasitic source-gate current leakage I_{SG} , and the decrease of the *ON/OFF* ratio. On the other hand the use of a high- k dielectric would induce an increase in the charge carrier localization. This effect is induced by the electronic polarization and by the decrease of the source-drain current I_{DS} . Veres *et al.* [87] have later investigated the effect of using a series of gate dielectrics with various polarities. They demonstrated that the transistor performances were considerably improved when gate dielectrics with a low permittivity of $k < 2.5$ were being used. According to the model introduced by the authors, the more polar would be the interface dielectric/semiconductor the more it would induce a broadening of the DOS leading to an increase of tail states.

Another approach to explain the role of the polar molecules present at dielectric/semiconductor interface was proposed by Sworakowski [86]. Indeed, the polar molecules create dipolar traps in the adjacent layer of the semiconductor. This results in a reduction of the charge carrier mobility extracted from the OTFT characteristics. However, since the depth of these traps decreases with the distance from the interface, a gradient of charge carrier mobility appears. The mobility in the region close to the dielectric appears lower than in the bulk. This effect can sometimes explain the gate voltage dependence on the mobility, or the difference between the turn-on and the threshold voltages.

The localisation effect of the charge carriers, induced by the high- k gate dielectric, can be reduced by covering the dielectric surface with an ultrathin self-assembled mono- or multilayer (SAMs or SAMTs). It has been demonstrated that SAMs show a relatively low leakage current of $\sim 10^{-8}$ A/cm², which is much lower than that for an ultrathin (few nm) SiO₂ layers. Long SAMs alkyl chains would act as spacers, separating the semiconductor from the dipoles in the dielectric. When using high- k hybrid dielectrics (polymer composites with high- k oxide nanoparticles), a similar effect could be achieved by covering the dielectric surface with a thin layer of pure polymer (for review please refer to [17]).

The ability of dipoles situated in the gate dielectric to create traps, inspired Sworakowski and coworkers to create an opto-electrical switch device using photochromic dielectric layers [93]. They developed a transistor made of perylene derivatives that were used as n -type semiconductors. The gate dielectric was made of poly(methyl methacrylate) with a dissolved photochromic material (spiropyran). The spiropyran molecules exhibited a large difference in the dipole moments of their stable and metastable forms. Hence, when illuminated with a UV light, an increase of the I_{DS} current and a decrease of the threshold voltage V_{th} was observed. These effects were reversible, and the initial parameters were restored by using thermal relaxation in the dark or by illuminating under the visible light.

Surface roughness of the dielectric

The roughness of the dielectric layer can disturb the molecular ordering of the deposited organic semiconductor and therefore introduce dislocations and structural traps. The unevenness of the dielectric polymer surface can exceed ten nm. Hence, in order to avoid deleterious effect on the charge carrier transport, one could design transistors with a top gate configuration. In this case the dielectric is deposited on a semiconducting layer which was previously formed without any structural defects on a smooth substrate [17]. Such a solution is however not universal, since semiconducting layers, especially when deposited from solutions, have very uneven surfaces. Another approach was introduced by Hwang *et al.* [94] who improved the surface smoothness and the transistor performances by covering the polymer dielectric films with a thin layer of metal oxide.

3.3.3. The main effects of charge carriers trapping on the performance of OTFTs

Häusermann *et al.* [95] extensively studied the influence of the trapping phenomenon on the current voltage characteristics of a very broad range of transistors. They analysed the normalized transfer curves of p - and n -type organic and inorganic transistors. The studies comprised organic single crystal transistors, evaporated small molecules thin-film transistors, inkjet printed polymer thin-film transistors and inorganic amorphous, polycrystalline tran-

sistors. These semiconductors were deposited on different dielectrics, including SiO_2 , SiN , Cytos. Sometimes the dielectric surface would be modified by SAMs. According to their analysis, the differences in the transient characteristics shapes resulted from the differences in deep trap densities in the semiconductors.

They claimed that the slope of the subthreshold region (given by the subthreshold swing SS , close to the turn-on voltage V_{ON} (see chapter 1.4 – Fig. 8(a) and Eq. (12)) is determined by the deep trap DOS. This applies when the Fermi level is far away from the transport level. Hence the highest the SS value would be, the fewer deep trap DOS will be observed. This was supported by several experimental evidences. For example, the organic single crystal transistors exhibit a very steep subthreshold region and a high mobility, whereas in the evaporated devices, the subthreshold is broad and the mobility is lower. Furthermore, the a-Si transistors, for both n - and p -type transports have a subthreshold region which is comparable to the evaporated transistors. They show a very low p -type transport mobility, but a high (up to $1 \text{ cm}^2/\text{Vs}$) n -type one. On the other hand, transistors with polycrystalline silicon exhibit a very high mobility, over $20 \text{ cm}^2/\text{Vs}$ (for both electrons and holes), but the broad subthreshold region indicates a high deep traps density.

The analysis of the dependences of the free charge carriers vs. the total charge carrier density showed that for transistors with single crystals the transport is very close to the theoretical trap-free limit. On the other hand, the transistors with evaporated layers are much more affected by the traps. The transistors with inkjet-printed polymers are situated in between the single crystals and the evaporated transistors. Interestingly, almost all inorganic transistors, with the exception of the n -type a-Si, are dominated by trap states.

4. CONCLUDING REMARKS

At the dawn of the organic semiconductors research, in 60-ties of XX century, the research was focused on understanding the basic physical rules governing the charge carrier generation and transport in organic materials. Experiments were performed on model molecular substances, usually in the form of single crystals with a controlled purity. This resulted in several fundamental models and theories describing the electrical and optoelectronic properties of the molecular materials [96]. The discovery of the so-called ‘synthetic metals’ and the conjugated polymers in the 70-ties was followed by a rapid development of the synthesis of countless other new organic semiconductors, conductors and even superconductors. This led in the last decade of XX century to the design of several organic electronic devices and to today’s emerging organic electronic technologies [1]. One could notice, that

unfortunately the development of new, often better, organic electronic devices is not always followed by basic researches with the aim to understand and describe the physical phenomena involved in such devices. By missing on this fundamental research point further progress could only be obtained via the less effective trial and error method.

An excellent example of a beneficial lesson which can be learned from basic models is the work published recently by Blom and coworkers [97]. They referred to some early work related to the charge carrier trapping phenomena [8, 98] and to space-charge limited current model elaborated by Mark and Helfrich [99]. From this model one could conclude, that the current in a semiconductor, scales with $N/(N_t)^r$, where N is the density of transporting sites, N_t is the density of trapping sites and the r exponent is a parameter dependent on the energy distribution of traps. When r is higher than 1 (as it is for deep or energetically distributed traps) one can anticipate that by diluting the semiconductor containing traps, both N and N_t will be proportionally reduced, and the resulting current density would increase. The authors showed that indeed such counterintuitive effect could be observed, by blending the conjugated polymer, poly[2-methoxy-5-(2-ethylhexyloxy)-1,4-phenylenevinylene] (MEH-PPV) with PVK. They found, that in the (MEH-PPV):(PVK) 1:9 blend the electron trapping was effectively eliminated, moreover the light-emitting diode made of this blend shows almost two times higher luminous efficiency when compared with a diode made of pure MEH-PPV.

We believe that this review related to the impact of charge carrier trapping on the performance of organic electronic devices, in particular organic light emitting diodes, highlights the importance of basic physical processes investigations in the field of organic electronics.

ACKNOWLEDGEMENTS

This work was supported by the European Union in frame of the grant Excilight, H2020-MSCA-ITN-2015, and by Polish National Research Centre in frame of the grants 2013/09/B/ST5/03521 and 2013/08/M/ST5/00914. A. L., B. G. R. D and J. U. acknowledge financial support by Foundation for Polish Science, grant Master 9./2014.

REFERENCE

- [1] Kohler, A.; Bässler H. *Electronic Processes in Organic Semiconductors: An Introduction*; Wiley-VCH, 2015.
- [2] Ku C. C. and Liepens R. *Electrical Properties of Polymers: Chemical Principles*; Hanser Publishers, Munich, 1987.

- [3] Hoesterey, D. C.; Letson, G. M. The Trapping of Photocarriers in Anthracene by Anthraquinone, Anthrone and Naphthacene, *J. Phys. Chem. Solids* **1963**, *24* (12), 1609–1615.
- [4] Nicolai, H. T.; Kuik, M.; Wetzelaer, G. A. H.; de Boer, B.; Campbell, C.; Risko, C.; Brédas, J. L.; Blom, P. W. M.; Unification of Trap-Limited Electron Transport in Semiconducting Polymers, *Nat. Mater.* **2012**, *11* (10), 882–887.
- [5] Dobruchowska, E.; Okrasa, L.; Glowacki, I.; Ulanski, J.; Boiteux, G.; The “Wet Dog” Effect in Polymers as Seen by Thermoluminescence, *Polymer* **2004**, *45* (17), 6027–6035.
- [6] So, F. *Organic Electronics: Materials, Processing, Devices and Applications*; CRC Press Taylor and Francis Group, Boca Raton, 2010.
- [7] Li, Z.; Meng, H.; *Organic Light-Emitting Materials and Devices*, CRC Press Taylor and Francis Group, Boca Raton, 2007.
- [8] Sworakowski, J.; On the Origin of Trapping Centres in Organic Molecular Crystals, *Mol. Cryst. Liq. Cryst.* **1970**, *11* (1), 1–11.
- [9] Young, R. H.; Sinicropi, J. A.; Fitzgerald, J. J.; Dipole Moments, Energetic Disorder, and Charge Transport in Molecularly Doped Polymers, *J. Phys. Chem.* **1995**, *99* (23), 9497–9506.
- [10] Borsenberger, P. M.; Gruenbaum, W. T., Electron Transport in a Molecularly Doped Polymer, *J. Polym. Sci. Part B Polym. Phys.* **1996**, *34* (3), 575–582.
- [11] Wolf, U., Bäessler, H.; Borsenberger, P. M.; Gruenbaum, W. T.; Hole Trapping in Molecularly Doped Polymers, *Chem. Phys.* **1997**, *222* (2–3), 259–267.
- [12] Nešpůrek, S., Sworakowski, J., Kadashchuk, A.; The Influence of Dipolar Species on Charge Carrier Transport in a Linear Polysilicon, *IEEE Trans. on Dielectrics and Electr. Insul.* **2001**, *8*, 432–441.
- [13] Chen, S.; Wu, Q.; Kong, M.; Zhao, X.; Yu, Z.; Jia, P.; Huang, W.; On the Origin of the Shift in Color in White Organic Light-Emitting Diodes, *J. Mater. Chem. C* **2013**, *1* (22), 3508–3524.
- [14] Yang, X.; Loos, J.; Toward High-Performance Polymer Solar Cells: The Importance of Morphology Control, *Macromolecules* **2007**, *40* (5), 1353–1362.
- [15] Nam, C.-Y.; Su, D.; Black, C. T.; High-Performance Air-Processed Polymer–Fullerene Bulk Heterojunction Solar Cells, *Adv. Funct. Mater.* **2009**, *19*, 3552–3559.
- [16] Newman, C. R.; Frisbie, C. D.; da Silva Filho, D. A.; Brédas, J.-L.; Ewbank, P. C.; Mann, K. R.; Introduction to Organic Thin Film Transistors and Design of N-Channel Organic Semiconductors, *Chem. Mater.* **2004**, *16* (23), 4436–4451.
- [17] Ortiz, R. P.; Facchetti, A.; Marks, T. J.; High- K Organic, Inorganic, and Hybrid Dielectrics for Low-Voltage Organic Field-Effect Transistors, *Chem. Rev.* **2010**, *110* (1), 205–239.
- [18] Takagi, K.; Nagase, T.; Kobayashi, T.; Naito, H.; Determination of Deep Trapping Lifetime in Organic Semiconductors Using Impedance Spectroscopy, *Appl. Phys. Lett.* **2016**, *108* (5), 53305.
- [19] Lang, D. V.; Deep-Level Transient Spectroscopy: A New Method to Characterize Traps in Semiconductors, *J. Appl. Phys.* **1974**, *45* (7), 3023.
- [20] Gaudin, O.; Jackman, R. B.; Nguyen, T.-P.; Le Rendu, P.; Determination of Traps in Poly(p-Phenylene Vinylene) Light Emitting Diodes by Charge-Based Deep Level Transient Spectroscopy, *J. Appl. Phys.* **2001**, *90* (8), 4196.
- [21] Kuik, M.; Vandenberg, J.; Goris, L.; Begemann, E. J.; Lutsen, L.; Vanderzande, D. J. M.; Manca, J. V.; Blom, P. W. M.; Optical Detection of Deep Electron Traps in Poly(p-phenylene vinylene) Light-Emitting Diodes, *Appl. Phys. Lett.* **2011**, *99* (18), 183305.
- [22] Mikla, V. I. and Mikla, V. V.; *Trap Level Spectroscopy in Amorphous Semiconductors*; Elsevier, London, 2010.
- [23] Simmons, J. G.; Taylor, G. W.; High-Field Isothermal Currents and Thermally Stimulated Currents in Insulators Having Discrete Trapping Levels, *Phys. Rev. B* **1972**, *5* (4), 1619–1629.
- [24] Werner, A. G.; Blochwitz, J.; Pfeiffer, M.; Leo, K.; Field Dependence of Thermally Stimulated Currents in Alq₃, *J. Appl. Phys.* **2001**, *90* (1), 123.
- [25] Steiger, J.; Schmechel, R.; von Seggern, H.; Energetic Trap Distributions in Organic Semiconductors, *Synth. Met.* **2002**, *129* (1), 1–7.

- [26] Chen, R. and Kirsh, Y. *Analysis of Thermally Stimulated Processes*, 1st ed.; Pergamon Press, Oxford, 1981.
- [27] Schmechel, R.; von Seggern, H.; Electronic Traps in Organic Transport Layers, *Phys. status solidi* **2004**, *201* (6), 1215–1235.
- [28] Urbach, F.; Stimulation von ZnS-Phosphoren Mit Temperature, *Wien. Berichte* **1930**, *139*, 363.
- [29] Glowacki, I.; Ulanski, J.; Simultaneous Measurements of Thermoluminescence and Thermally Stimulated Currents in Poly(N-vinylcarbazole)/polycarbonate Blends, *J. Appl. Phys.* **1995**, *78* (2), 1019–1025.
- [30] Ulanski, J.; Sielski, J.; Glowacki, I.; Kryszewski, M.; Transition from Dispersive to Non-Dispersive Hole Transport in Poly-N-vinylcarbazole/polycarbonate Mixtures, *IEEE Trans. Electr. Insul.* **1992**, *27* (4), 714–718.
- [31] Samoc, M.; Samoc, A.; Sworakowski, J.; Karl, N.; TSC Transport Peak in Phenothiazine-Doped Anthracene Crystals, *J. Phys. C Solid State Phys.* **1983**, *16* (1), 171–180.
- [32] Zielinski, M.; Samoc, M.; An Investigation of the Poole-Frenkel Effect by the Thermally Stimulated Current Technique, *J. Phys. D. Appl. Phys.* **1977**, *10* (8), L105–L107.
- [33] Plans, J.; Application of the Onsager Theory to Thermally Stimulated Currents, *J. Appl. Phys.* **1982**, *53* (4), 3103.
- [34] Garlick, G. F. J.; Gibson, A. F.; The Electron Trap Mechanism of Luminescence in Sulphide and Silicate Phosphors, *Proc. Phys. Soc.* **1948**, *60* (6), 574–590.
- [35] Glowacki, I.; Szamel, Z.; The Nature of Trapping Sites and Recombination Centres in PVK and PVK–PBD Electroluminescent Matrices Seen by Spectrally Resolved Thermoluminescence, *J. Phys. D. Appl. Phys.* **2010**, *43* (29), 295101 (9pp), doi:10.1088/0022-3727/43/29/295101.
- [36] Kao, K.-C.; Hwang W.; *Electrical Transport in Solids: With Particular Reference to Organic Semiconductors*, 1st ed.; Pergamon Press, Oxford, 1981.
- [37] Moliton, A.; Nunzi, J.-M.; How to Model the Behaviour of Organic Photovoltaic Cells, *Polym. Int.* **2006**, *55* (6), 583–600.
- [38] Murgatroyd, P. N.; Theory of Space-Charge-Limited Current Enhanced by Frenkel Effect, *J. Phys. D. Appl. Phys.* **1970**, *3* (2), 151.
- [39] Mark, P.; Helfrich, W.; Space-Charge-Limited Currents in Organic Crystals, *J. Appl. Phys.* **1962**, *33* (1), 205.
- [40] Tanase, C.; Meijer, E. J.; Blom, P. W. M.; de Leeuw, D. M.; Unification of the Hole Transport in Polymeric Field-Effect Transistors and Light-Emitting Diodes, *Phys. Rev. Lett.* **2003**, *91* (21), 216601.
- [41] Pasveer, W. F.; Cottaar, J.; Tanase, C.; Coehoorn, R.; Bobbert, P. A.; Blom, P. W. M.; de Leeuw, D. M.; Michels, M. A. J.; Unified Description of Charge-Carrier Mobilities in Disordered Semiconducting Polymers, *Phys. Rev. Lett.* **2005**, *94* (20), 206601.
- [42] Nicolai, H. T.; Mandoc, M. M.; Blom, P. W. M.; Electron Traps in Semiconducting Polymers: Exponential versus Gaussian Trap Distribution, *Phys. Rev. B* **2011**, *83* (19), 195204.
- [43] Estrada, M.; Cerdeira, A.; Puigdollers, J.; Reséndiz, L.; Pallares, J.; Marsal, L. F.; Voz, C.; Iñiguez, B.; Accurate Modeling and Parameter Extraction Method for Organic TFTs, *Solid. State. Electron.* **2005**, *49* (6), 1009–1016.
- [44] Wondmagegn, W.; Pieper, R.; Simulation of Top-Contact Pentacene Thin Film Transistor, *J. Comput. Electron.* **2009**, *8* (1), 19–24.
- [45] Ng, K. K.; *Complete Guide to Semiconductor Devices*; John Wiley & Sons, Inc., New York, 2002.
- [46] Mao, L.-K.; Hwang, J.-C.; Chang, T.-H.; Hsieh, C.-Y.; Tsai, L.-S.; Chueh, Y.-L.; Hsu, S. S. H.; Lyu, P.-C.; Liu, T.-J.; Pentacene Organic Thin-Film Transistors with Solution-Based Gelatin Dielectric, *Org. Electron.* **2013**, *14* (4), 1170–1176.
- [47] Romaner, L.; Pogantsch, A.; Scanducci de Freitas, P.; Scherf, U.; Gaal, M.; Zojer, E.; List, E. J. W.; The Origin of Green Emission in Polyfluorene-Based Conjugated Polymers: On-Chain Defect Fluorescence, *Adv. Funct. Mater.* **2003**, *13* (8), 597–601.

- [48] Sainova, D.; Miteva, T.; Nothofer, H. G.; Scherf, U.; Glowacki, I.; Ulanski, J.; Fujikawa, H.; Neher, D.; Control of Color and Efficiency of Light-Emitting Diodes Based on Polyfluorenes Blended with Hole-Transporting Molecules, *Appl. Phys. Lett.* **2000**, *76* (14), 1810.
- [49] Sainova, D.; Neher, D.; Dobruchowska, E.; Luszczynska, B.; Glowacki, I.; Ulanski, J.; Nothofer, H.-G.; Scherf, U.; Thermoluminescence and Electroluminescence of Annealed Polyfluorene Layers, *Chem. Phys. Lett.* **2003**, *371* (1–2), 15–22.
- [50] Fishchuk, I. I.; Kadashchuk, A. K.; Vakhnin, A.; Korosko, Y.; Bäessler, H.; Souharce, B.; Scherf, U.; Transition from Trap-Controlled to Trap-to-Trap Hopping Transport in Disordered Organic Semiconductors, *Phys. Rev. B* **2006**, *73* (11), 115210.
- [51] Luszczynska, B.; Dobruchowska, E.; Glowacki, I.; Ulanski, J.; Ego, Ch.; Grimsdale, A. C.; Müllen, K.; Influence of Physical and Chemical Modification on Charge Carrier Trapping and Recombination Processes in Polyfluorenes, *J. Nanostruct. Polym. Nanocomp.* **2007**, *3* (4), 125–135.
- [52] Luszczynska, B.; Dobruchowska, E.; Glowacki, I.; Danel, A.; Ulanski, J.; Thermoluminescence of the Blue Light-Emitting System Based on Poly(9-vinylcarbazole) Doped with a Pyrazoloquinoline Dye, *J. Lumin.* **2009**, *129* (10), 1215–1218.
- [53] Arkhipov, V. I.; Emelianova, E. V.; Kadashchuk, A.; Blonsky, I.; Nešpurenk, S.; Weiss, D. S.; Bäessler, H.; Polaron Effects on Thermally Stimulated Photoluminescence in Disordered Organic Systems, *Phys. Rev. B* **2002**, *65* (16), 165218.
- [54] Kadashchuk, A.; Skryshevskii, Y.; Vakhnin, A.; Ostapenko, N.; Arkhipov, V. I.; Emelianova, E. V.; Bäessler, H.; Thermally Stimulated Photoluminescence in Disordered Organic Materials, *Phys. Rev. B* **2001**, *63* (11), 115205.
- [55] Richert, R.; Blumen, A.; *Disorder Effects on Relaxational Processes*; Springer, Berlin, 1994.
- [56] Bäessler, H.; Localized States and Electronic Transport in Single Component Organic Solids with Diagonal Disorder, *Phys. status solidi* **1981**, *107* (1), 9–54.
- [57] Glowacki, I.; Szamel, Z.; The Impact of 1wt% of Ir(ppy)₃ on Trapping Sites and Radiative Recombination Centres in PVK and PVK/PBD Blend Seen by Thermoluminescence, *Org. Electron.* **2015**, *24*, 288–296.
- [58] Al-Attar, H. A.; Griffiths, G. C.; Moore, T. N.; Tavasli, M.; Fox, M. A.; Bryce, M. R.; Monkman, A. P.; Highly Efficient, Solution-Processed, Single-Layer, Electrophosphorescent Diodes and the Effect of Molecular Dipole Moment, *Adv. Funct. Mater.* **2011**, *21* (12), 2376–2382.
- [59] Kadashchuk, A. K.; Ostapenko, N. I.; Lukashenko, N. V.; On the Application of Thermoluminescence for Probing the Energetic Disorder in Amorphous Molecular Solids, *Adv. Mater. Opt. Electron.* **1997**, *7*, 99–103.
- [60] Glowacki, I.; Szamel, Z.; Wiosna-Salyga, G.; Spectrally Resolved Thermoluminescence versus Electroluminescence Spectra of PVK Doped with 1 wt % of Ir(btpp)₂(acac), *Org. Electron.* **2016**, *31*, 127–135.
- [61] Kadashchuk, A.; Schols, S.; Vakhnin, A.; Genoe, J.; Heremans, P.; Triplet Dynamics and Charge Carrier Trapping in Triplet-Emitter Doped Conjugated Polymers, *Chem. Phys.* **2009**, *358* (1–2), 147–155.
- [62] Glowacki, I.; Szamel, Z.; Wiosna-Salyga, G.; Blue Iridium Complexes as Electron Trapping Sites and Efficient Recombination Centres in Poly(N-vinylcarbazole) Seen by Spectrally Resolved Thermoluminescence, *Synth. Met.* **2016**, *220*, 213–220.
- [63] Kawamura, Y.; Goushi, K.; Brooks, J.; Brown, J. J.; Sasabe, H.; Adachi, C.; 100% Phosphorescence Quantum Efficiency of Ir(III) Complexes in Organic Semiconductor Films, *Appl. Phys. Lett.* **2005**, *86* (7), 71104.
- [64] Lenkeviciute, B.; Vitkus, M.; Juska, G.; Genevicius, K.; Hybrid OLEDs with CdSse1-x/ZnS Core-shell Quantum Dots: An Investigation of Electroluminescence Properties, *Synth. Met.* **2015**, *209*, 343–347.
- [65] Tessler, N.; Preezant, Y.; Rappaport, N.; Roichman, Y.; Charge Transport in Disordered Organic Materials and Its Relevance to Thin-Film Devices: A Tutorial Review, *Adv. Mater.* **2009**, *21* (27), 2741–2761.

- [66] Giebink, N. C.; Wiederrecht, G. P.; Wasielewski, M. R.; Forrest, S. R.; Ideal Diode Equation for Organic Heterojunctions, Derivation and Application. *Phys. Rev. B* **2010**, *82* (15), 155305.
- [67] Kirchartz, T.; Deledalle, F.; Tuladhar, P. S.; Durrant, J. R.; Nelson, J.; On the Differences between Dark and Light Ideality Factor in Polymer:Fullerene Solar Cells, *J. Phys. Chem. Lett.* **2013**, *4* (14), 2371–2376.
- [68] Mandoc, M. M.; Kooistra, F. B.; Hummelen, J. C.; de Boer, B.; Blom, P. W. M.; Effect of Traps on the Performance of Bulk Heterojunction Organic Solar Cells, *Appl. Phys. Lett.* **2007**, *91* (26), 263505.
- [69] Cowan, S. R.; Leong, W. L.; Banerji, N.; Dennler, G.; Heeger, A. J.; Identifying a Threshold Impurity Level for Organic Solar Cells: Enhanced First-Order Recombination Via Well-Defined PC₈₄BM Traps in Organic Bulk Heterojunction Solar Cells, *Adv. Funct. Mater.* **2011**, *21* (16), 3083–3092.
- [70] Shockley, W.; Read, W. T.; Statistics of the Recombinations of Holes and Electrons, *Phys. Rev.* **1952**, *87* (5), 835–842.
- [71] Hall, R. N.; Electron-Hole Recombination in Germanium, *Phys. Rev.* **1952**, *87* (2), 387–387.
- [72] Sworakowski, J.; Lipiński, J.; Janus, K.; On the Reliability of Determination of Energies of HOMO and LUMO Levels in Organic Semiconductors from Electrochemical Measurements. A Simple Picture Based on the Electrostatic Model, *Org. Electron.* **2016**, *33* (2), 300–310.
- [73] Street, R. A.; Electronic Structure and Properties of Organic Bulk-Heterojunction Interfaces, *Adv. Mater.* **2016**, *28* (20), 3814–3830.
- [74] Garcia-Belmonte, G.; Boix, P. P.; Bisquert, J.; Lenes, M.; Bolink, H. J.; La Rosa, A.; Filippone, S.; Martín, N.; Influence of the Intermediate Density-of-States Occupancy on Open-Circuit Voltage of Bulk Heterojunction Solar Cells with Different Fullerene Acceptors, *J. Phys. Chem. Lett.* **2010**, *1* (17), 2566–2571.
- [75] Horowitz, G.; Hajlaoui, R.; Bourguiga, R.; Hajlaoui, M.; Theory of the Organic Field-Effect Transistor, *Synth. Met.* **1999**, *101* (1–3), 401–404.
- [76] Mottaghi, M.; Horowitz, G.; Field-Induced Mobility Degradation in Pentacene Thin-Film Transistors, *Org. Electron.* **2006**, *7* (6), 528–536.
- [77] Donley, C. L.; Zaumseil, J.; Andreasen, J. W.; Nielsen, M. M.; Sirringhaus, H.; Friend, R. H.; Kim, J.-S.; Effects of Packing Structure on the Optoelectronic and Charge Transport Properties in Poly(9,9-di-n-octylfluorene-alt-benzothiadiazole), *J. Am. Chem. Soc.* **2005**, *127* (37), 12890–12899.
- [78] Kleinhenz, N.; Persson, N.; Xue, Z.; Chu, P. H.; Wang, G.; Yuan, Z.; McBride, M. A.; Choi, D.; Grover, M. A.; Reichmanis, E.; Ordering of Poly(3-hexylthiophene) in Solutions and Films: Effects of Fiber Length and Grain Boundaries on Anisotropy and Mobility, *Chem. Mater.* **2016**, *28* (11), 3905–3913.
- [79] Dimitrakopoulos, C. D.; Malenfant, P. R. L.; Organic Thin Film Transistors for Large Area Electronics, *Adv. Mater.* **2002**, *14* (2), 99–117.
- [80] Miskiewicz, P.; Mas-Torrent, M.; Jung, J.; Kotarba, S.; Glowacki, I.; Gomar-Nadal, E.; Amabilino, D. B.; Veciana, J.; Krause, B.; Carbone, D.; Rovira, C.; Ulanski, J.; Efficient High Area OFETs by Solution Based Processing of a π -Electron Rich Donor, *Chem. Mater.* **2006**, *18* (20), 4724–4729.
- [81] Tszydyl, I.; Kucinska, M.; Marszalek, T.; Rybakiewicz, R.; Nosal, A.; Jung, J.; Gazicki-Lipman, M.; Pitsalidis, C.; Gravalidis, C.; Logothetidis, S.; Zagorska, M.; Ulanski, J.; High-Mobility and Low Turn-On Voltage N-Channel OTFTs Based on a Solution-Processable Derivative of Naphthalene Bisimide, *Adv. Funct. Mater.* **2012**, *22* (18), 3840–3844.
- [82] Sirringhaus, H.; Brown, P. J.; Friend, R. H.; Nielsen, M. M.; Bechgaard, K.; Langeveld-Voss, B. M. W.; Spiering, A. J. H.; Janssen, R. A. J.; Meijer, E. W.; Herwig, P.; de Leeuw, D. M.; Two-Dimensional Charge Transport in Self-Organized, High-Mobility Conjugated Polymers, *Nature* **1999**, *401* (6754), 685–688.

- [83] Janasz, L.; Chlebosz, D.; Gradzka, M.; Zajaczkowski, W.; Marszalek, T.; Müllen, K.; Ulanski, J.; Kiersnowski, A.; Pisula, W.; Improved Charge Transport in Ultrathin Poly(3-hexylthiophene) Films via Solution Aggregation, *J. Mat. Chem. C* **2016**, *4*, 11488–11498.
- [84] Najafov, H.; Mastrogiovanni, D.; Garfunkel, E.; Feldman, L. C.; Podzorov, V.; Photon-Assisted Oxygen Diffusion and Oxygen-Related Traps in Organic Semiconductors, *Adv. Mater.* **2011**, *23* (8), 981–985.
- [85] Li, D.; Borkent, E.-J.; Nortrup, R.; Moon, H.; Katz, H.; Bao, Z.; Humidity Effect on Electrical Performance of Organic Thin-Film Transistors, *Appl. Phys. Lett.* **2005**, *86* (4), 42105.
- [86] Sworakowski, J.; Current-voltage Characteristics in Organic Field-Effect Transistors. Effect of Interface Dipoles, *Chem. Phys.* **2015**, *456*, 106–110.
- [87] Veres, J.; Ogier, S. D.; Leeming, S. W.; Cupertino, D. C.; Mohialdin Khaffaf, S.; Low-K Insulators as the Choice of Dielectrics in Organic Field-Effect Transistors, *Adv. Funct. Mater.* **2003**, *13* (3), 199–204.
- [88] Sharma, A.; Mathijssen, S. G. J.; Bobbert, P. A.; de Leeuw, D. M.; Influence of the Semiconductor Oxidation Potential on the Operational Stability of Organic Field-Effect Transistors, *Appl. Phys. Lett.* **2011**, *99* (10), 103302.
- [89] Mathijssen, S. G. J.; Spijkman, M.-J.; Andringa, A.-M.; van Hal, P. A.; McCulloch, I.; Kemerink, M.; Janssen, R. A. J.; de Leeuw, D. M.; Revealing Buried Interfaces to Understand the Origins of Threshold Voltage Shifts in Organic Field-Effect Transistors, *Adv. Mater.* **2010**, *22* (45), 5105–5109.
- [90] Tszydyl, I.; Marszalek, T.; Ulanski, J.; Nosal, A.; Gazicki-Lipman, M.; Applications of Parylene Films in the Manufacture of Organic Field-Effect Transistors, *Surf. Coatings Technol.* **2016**, *290*, 21–27.
- [91] Pfatner, R.; Mas-Torrent, M.; Bilotti, I.; Brillante, A.; Milita, S.; Liscio, F.; Biscarini, F.; Marszalek, T.; Ulanski, J.; Nosal, A.; Gazicki-Lipman, M.; Leufgen, M.; Schmidt, G.; Molenkamp, L. W.; Laukhin, V.; Veciana, J.; Rovira, C.; High-Performance Single Crystal Organic Field-Effect Transistors Based on Two Dithiophene-Tetrathiafulvalene (DT-TTF) Polymorphs, *Adv. Mater.* **2010**, *22* (37), 4198–4203.
- [92] Wang, A.; Kymissis, I.; Bulovic, V.; Akinwande, A. I.; Engineering Density of Semiconductor-Dielectric Interface States to Modulate Threshold Voltage in OFETs, *IEEE Trans. Electron Devices* **2006**, *53* (1), 9–13.
- [93] Lutsyk, P.; Janus, K.; Sworakowski, J.; Generali, G.; Capelli, R.; Muccini, M.; Photo-switching of an N-Type Organic Field Effect Transistor by a Reversible Photochromic Reaction in the Dielectric Film, *J. Phys. Chem. C* **2011**, *115* (7), 3106–3114.
- [94] Hwang, D. K.; Kim, C. S.; Choi, J. M.; Lee, K.; Park, J. H.; Kim, E.; Baik, H. K.; Kim, J. H.; Im, S.; Polymer/YOx Hybrid-Sandwich Gate Dielectrics for Semitransparent Pentacene Thin-Film Transistors Operating Under 5 V, *Adv. Mater.* **2006**, *18* (17), 2299–2303.
- [95] Häusermann, R.; Willa, K.; Blülle, B.; Morf, T.; Facchetti, A.; Chen, Z.; Lee, J.; Batlogg, B.; Device Performance and Density of Trap States of Organic and Inorganic Field-Effect Transistors, *Org. Electron.* **2016**, *28*, 306–313.
- [96] Pope, M.; Swenberg, C. E.; *Electronic Processes in Organic Crystals and Polymers*; Oxford University Press, 1999.
- [97] Abbaszadeh, D.; Kunz, A.; Wetzelaer, G. A. H.; Michels, J. J.; Cra ciun, N. I.; Koynov, K.; Lieberwirth, I.; Blom, P. W. M.; Elimination of Charge Carrier Trapping in Diluted Semiconductors, *Nat. Mater.* **2016**, *15* (6), 628–633.
- [98] Rose, A.; Recombination Processes in Insulators and Semiconductors, *Phys. Rev.* **1955**, *97* (2), 322–333.
- [99] Mark, P.; Helfrich, W.; Space-Charge-Limited Currents in Organic Crystals, *J. Appl. Phys.* **1962**, *33* (1), 205–215.